Chemical and Process Engineering: New Frontiers, 2026, 47(2), e132
DOI: 10.24425/cpe.2026.158130

CRITICAL REVIEW

Cathode and anode materials for alkali metal electrochemical reactions in energy storage systems – current state of the art and potential developments

Wojciech Rejmer[1], Szymon Racewicz[2,*], Sławomir Wierzbicki[2]

[1] University of Warmia and Mazury in Olsztyn, Faculty of Technical Sciences, Department of Materials and Machines Technology, Oczapowskiego 11, Olsztyn, Poland
[2] University of Warmia and Mazury in Olsztyn, Faculty of Technical Sciences, Department of Mechatronics, Oczapowskiego 11, Olsztyn, Poland

* **Corresponding author, e-mail:** szymon.racewicz@uwm.edu.pl

Article info:
Received: 15 January 2026
Revised: 21 April 2026
Accepted: 06 May 2026

Abstract
European and world economies are displaying increased use of renewable energy sources (RES). Energy sources such as wind energy, solar energy and water current energy, while clean and not emitting carbon dioxide, do not allow for stable electrical energy production due to their dependence on weather conditions. Current development trends are focused on the production of energy storage units, which will allow for stable electricity production from renewable sources. One unit investigated by researchers is flow and steady state high-capacity batteries. Ideal storage system should be characterised by high electric stability, charge-discharge reversibility, stability and low cost. The most widely used technology is ion lithium batteries. However, sources of lithium are geographically and quantitatively limited. There is an increasing interest in the application of other active metals in energy storage systems. Most active metal salts exhibit high water solubility and are available in most parts of the world. The objective of this work was to catalogue known active metals usage in energy storage, including their current and most promising applications, with a focus on the capacity of electrochemical processes and on anode and cathode materials.

Keywords
energy storage, renewable sources, active metals, cathodes, anodes

1. RENEWABLE ENERGY SOURCES

Current discussion on climate change, both in the European Union and the world, leads to increasing implementation of RES. The most common non-emissive energy sources are solar energy, wind energy, hydroelectric power, and geothermal energy (Nazarov et al., 2024). Solar power is divided into active and passive technologies, and active technologies are divided into concentrated solar power and photovoltaic technologies. Active solar power sources are those that convert heat or solar irradiation into electric energy. Their current efficiency ranges from 13 to 30% (Shahabuddin et al., 2021). To utilise solar energy technology in electrical grids, energy storage systems are paramount. The objective is to capture the excess generated electric energy and use it in times of energy generation decline.

Extensive investigations have underscored the critical role of electrochemical energy storage technologies in enhancing the overall efficiency and utilisation of photovoltaic systems. According to data published by the International Renewable Energy Agency (IRENA), the integration of energy storage systems can elevate the self-consumption rate of solar-generated electricity to approximately 50%, while concurrently mitigating dependence on the electrical grid and minimising curtailment of photovoltaic output (IRENA, 2017).

In recent years, stringent environmental legislation implemented in both the United States and the European Union has mandated reductions in anthropogenic greenhouse gas emissions in the order of 20–30%. These regulatory frameworks actively incentivise the large-scale deployment of RES, thereby driving accelerated expansion of the global battery market (Kim and Lee, 2024).

2. ENERGY STORAGE SYSTEMS

Rechargeable battery-based storage systems, such as lithium-ion batteries, are of considerable interest because of their high energy density, efficiency, and cost-effectiveness (Bustos et al., 2023; Hong et al., 2023). Rechargeable batteries, also called storage batteries or secondary cells, are electrochemical systems that use reversible redox reactions, which allow for multiple charging and recharging cycles. This is opposed to primary cells that have only one discharge cycle due to one of the reaction products being gaseous or unstable. Rechargeable systems store electrical energy employing conjugated electronation and de-electronation chemical reactions and release it in the same manner when needed (Lung et al., 2023). Evaluation research was performed considering the performance of a lithium-ion battery energy storage system

integrated with solar PV installations. It has been found that the self-consumption of solar energy was improved by 30% and the reliance on grid electricity was reduced with the implementation of lithium-ion batteries (Vieira et al., 2017). Another research (Roberts et al., 2019) analysed the performance of a battery energy storage system (BESS) integrated with a solar PV system. In this study, it was concluded that the BESS increased the self-consumption of solar energy to over 70%, resulting in a significant reduction in grid electricity purchases. The techno-economic performance of a lithium-ion battery was evaluated in another study (Hassan et al., 2024) as an application for a solar self-consumption energy storage system. Other studies also showed improvement in self-consumption and economic efficiency of solar systems (Hasan et al., 2023). Presented research shows that integration of energy storage systems with PV installations is economically viable, underscoring the need for further development in this field. Because of this fact, it is crucial to develop storage systems based on a wider resource base. For this reason, energy storage systems based on alkali metals have been recognised by European markets due to their strong reliance on the foreign supply of both raw materials and end products, especially from Asia (Nowaczek and Kulczycka, 2020).

Although energy storage technologies have evolved in recent years, their main principles have not changed. The chemical energy storage systems are used mostly in the consumer sector and infrastructure maintenance (Komarnicki, 2016). Battery technology advancement has been revolutionised by portable electronics. This advancement has led to battery usage on demand and as a supply in fields like transportation or the electrical grid. Due to the high costs of power grid instabilities in the US, significant investments are being made (Amarapala et al., 2023). According to Jones Lang LaSalle Incorporated, utility-scale battery energy storage systems have reached the point of 16 GW in the USA by 2023, and their value worldwide can grow to 150 billion USD by the end of 2030 (JLL, 2024). The development and wide usage of lithium-ion batteries led to interest in other systems based on alkali metals such as sodium, potassium, magnesium, and calcium. Those metals are significantly close to lithium in the periodic table and are more abundant in Earth's crust. The amount of those elements is as follows (mass%): lithium is 0.002%, sodium is 2.36%, potassium is 2.09%, magnesium is 2.33% (Haynes et al., 2016; Lindagato et al., 2023) and calcium 4.15% (Royal Society of Chemistry) (Fig. 1). The main sources of lithium are places in Southeast Asia, Australia, and South America. Sodium and potassium are most abundant in North America (U.S. Geological Survey, 2020). Magnesium is most widespread but mostly produced in China and Russia (Zhang et al., 2023a). Calcium sources are most abundant in Indonesia, South America, and Central Africa (Wood et al., 2022). The new materials development for components of batteries (electrodes) is key to the improvement of battery performance and safety (Palumbo, 2023). Due to the anticipated increase in the usage of lithium-ion batteries, research on the recycling of materials from used systems is widely investigated (Barsegyan and Baghdasaryan, 2022; Huang et al., 2025; Kujawińska et al., 2022; Shim et al., 2024).

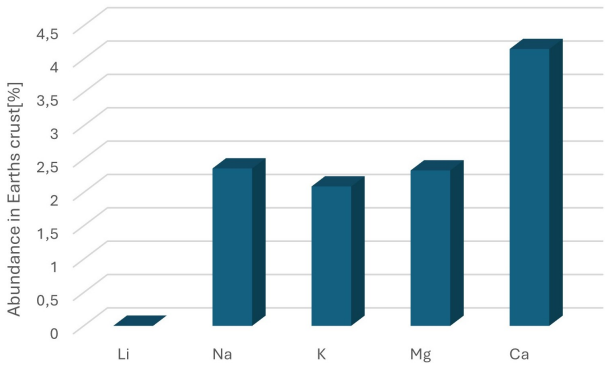

Figure 1. Abundance of lithium, sodium, potassium and magnesium in Earth's crust.

3. LITHIUM-ION BATTERIES (LIBS)

The prototype of lithium-ion batteries was introduced in 1986 by a research group of Akira Yoshino. The base principle of LIBs is the same as that of other alkali-ion batteries. Its core principle is reversible intercalation of ions, which began with research on the transport of ions in solids published in the 1960s (Lavanya et al., 2025), which was followed by investigation of reversible intercalation of lithium ions into graphite developed in the 1970s (Besenhard and Eichinger, 1976). In the same decade, the development of the first lithium metal battery occurred, thanks to the works of Whittingham, who developed the first lithium-ion rechargeable battery with titanium sulphide cathode. This set-up proved not sufficient for commercial use due to high material cost and hydrogen sulphide production during cathode decomposition (Whittingham, 1976). The end of the 70s saw the incorporation of lithium–transition metal oxides as cathodes, which proved more viable than titanium sulphide in works of Godshall (Godshall et al., 1980), Goodenough and Mizushima (Mizushima et al., 1980). A final development made by a group in the pre-commercialisation phase was the development of rechargeable batteries using ethyl carbonate as solvent, with $LiPF_6$ as electrolyte, which was Yoshino's group's prototype. Since then, the performance of lithium-ion cells has improved from a specific energy of 120 Wh/kg for the first Sony battery to 270 Wh/kg for current products (Waldmann et al., 2020). The remaining problem of LIBs is heat generation, which can be a reason for the proliferation of safety issues (fires and explosions included). Another problem is decreased performance with the lowering of temperature, which has been proven to reduce power outputs, life cycles and usable capacity (Xu et al., 2024).

The substantial annual production volumes of lithium-ion batteries, currently ranging from 1 to 10 GWh per manufacturing facility, necessitate the unequivocal demonstration of gigawatt-hour-scale production capability. Such a demonstration is

essential to satisfy the stringent qualification requirements imposed by automotive original equipment manufacturers (OEMs) and to ensure that the resulting cells achieve the cost-competitiveness required for widespread adoption (Nelson et al., 2011). Scale-up of production has precipitated a precipitous decline in specific cell costs, from approximately 5000 $/kWh in 1991 to 101 $/kWh in 2021 (Kittner et al., 2017; Ziegler and Trancik, 2021). This dramatic reduction underpinned the proliferation of portable electronic devices during the so-called "decade of the smartphone". Global demand for lithium-ion batteries expanded more than tenfold over the same period, rising from approximately 30 GWh in 2011 to 492 GWh in 2021, with projections indicating an increase to 2–3.5 TWh by 2030 (IEA, 2022). Sustained growth in demand is anticipated to drive further enhancements in electrochemical performance concomitant with additional price reductions. Advances in cell chemistry and architecture, battery-pack engineering, and manufacturing processes have collectively contributed to these improvements in energy density, cycle life, safety, and cost. At the inception of commercialisation in 1991, only cells employing lithium cobalt oxide ($LiCoO_2$, commonly abbreviated LCO) cathodes paired with graphitic carbon anodes were available on the market. In these early formulations, the active cathode material contained approximately 60 wt% of cobalt (Winter et al., 2018; Yűksel and Lale, 2024). According to the current research, the specific energy of lithium cells exceeds 270 Wh/kg (Sgourou et al., 2023). Positive electrode materials in such devices have high nickel and low cobalt content. Examples include lithium nickel manganese cobalt oxide ($LiNi_{1-a-b}Mn_aCo_bO_2$, where $a+b<1$, or $Ni_xMn_yCo_z$ where $x:y:z$ reflects the molar ratio of metals Ni:Mn:Co). Changes in positive electrode chemistry also led to improvements in both energy and cost effectiveness. Lithium iron phosphate ($LiFePO_4$, LFP)-based batteries employing a cell-to-pack (CTP) architecture have been implemented, achieving a gravimetric energy density of approximately 160 Wh/kg and a volumetric energy density of 330 Wh/l (Yang et al., 2021). These materials are safer and potentially cheaper (Wentker et al., 2019). The current generation of lithium-ion batteries, relying on intercalation-based cathodes, is approaching its theoretical performance limits. Accordingly, scientists are now directing attention towards alternative electrode materials and advanced processing techniques.

Key innovations include silicon-rich negative electrodes (Zhao et al., 2025), lithium-metal negative electrodes (Jeon et al., 2025), and solid-state electrolytes (Yun et al., 2024), negative electrode pre-lithiation strategies (Overhoff et al., 2021), and dry electrode coating processes (Park et al., 2025).

Emerging research directions in positive-electrode development focus on active materials that operate via conversion mechanisms, notably sulfur-based and oxygen-based systems. Although these chemistries offer potential advantages in raw-material cost and abundance, they typically compromise volumetric and gravimetric energy density, cycle life, and voltage stability compared with conventional intercalation hosts (Frith et al., 2023).

The fundamental energy-storage mechanism in lithium-ion batteries relies on reversible electrochemical insertion/extraction (intercalation/deintercalation) reactions. During charge, lithium ions are extracted from the crystal lattice of the cathode, migrate through the electrolyte and separator, and incorporate into the anode host structure. The reverse process occurs upon discharge. The reversible cell capacity is therefore governed by the number of lithium ions that can be accommodated per unit mass or volume within the respective electrode frameworks.

To tailor parameters such as energy density, power, safety, cost, and operating temperature range, diverse cathode and anode material pairings are employed. Widely commercialised cathode compositions include spinel lithium manganese oxide ($LiMn_2O_4$, LMO), olivine lithium iron phosphate ($LiFePO_4$, LFP), and layered nickel-cobalt-manganese oxides ($Li[Ni_xCo_yMn_{1-x-y}]O_2$, NCM or NMC). Common negative-electrode materials comprise graphite and spinel lithium titanate ($Li_4Ti_5O_{12}$, LTO).

Layered NCM cathodes are distinguished by their high theoretical specific capacity ($\approx$ 270–280 mAh/g when fully delithiated) (Ahangari et al., 2024; Hu et al., 2020), favourable rate capability, and respectable low-temperature kinetics. Performance can be further optimised by adjusting the transition-metal stoichiometry (Ni:Co:Mn ratio), wherein higher nickel content generally increases capacity at the expense of thermal stability and cycle life. In contrast, $LiFePO_4$ exhibits a lower practical specific capacity ($\approx$ 160–170 mAh/g) but offers intrinsic thermal and electrochemical stability, dramatically reducing the risk of oxygen release and thermal runaway even under abusive conditions such as overcharge (Hu et al., 2024; Lung-Hao Hu et al., 2013). Spinel LMO provides the lowest capacity among the three ($\approx$ 100–120 mAh/g practical) yet benefits from low material cost and environmental benignity (Abbas et al., 2024; Jiang et al., 2023).

On the anode side, graphite's highly ordered layered structure enables a high gravimetric capacity ($\approx$ 360–370 mAh/g via formation of LiC_6) and excellent performance rate. However, during the initial charge cycle, reductive decomposition of the electrolyte generates a solid-electrolyte interphase (SEI) layer on the graphite surface. Although this passivating film is essential for preventing continuous electrolyte degradation, it irreversibly consumes lithium and reduces overall cell capacity (Stournara and Shenoy, 2011; Xie and Lu, 2020). Lithium titanate, by contrast, operates at a higher potential ($\approx$ 1.55 V vs. Li/Li^+) outside the electrolyte reduction window, eliminating SEI formation and conferring exceptional safety and cycle life. These advantages come at the cost of substantially lower cell voltage and energy density, as well as higher material cost, restricting LTO deployment to niche applications demanding ultra-high safety and moderate energy requirements (Wang et al., 2017).

Commercially dominant cell chemistries remain limited to a few well-optimised pairings, including LFP/graphite,

LMO/graphite (or LMO-NCM blends), NCM/graphite, and LFP/LTO. Among these, NCM/graphite systems currently predominate in battery-electric passenger vehicles owing to their superior combination of gravimetric and volumetric energy density, high-rate capability, and acceptable low-temperature performance, all of which directly translate to extended driving range and dynamic vehicle performance (Yang et al., 2023).

3.1. Anodes for LIBs

The foundation of modern lithium-ion battery systems continues to rely on intercalation-based cathode and anode materials paired with non-aqueous liquid electrolytes, commonly comprising 1–1.2 M $LiPF_6$ in binary or multicomponent solvents of cyclic and chain alkyl carbonates (e.g., ethylene carbonate (EC) blended with dimethyl carbonate (DMC), diethyl carbonate (DEC), or ethyl methyl carbonate (EMC)). For more than a quarter of a century, graphite has served as the predominant anode material in commercial cells owing to its low average delithiation potential (≈ 0.1 V vs. Li/Li^+), high specific capacity of 372 mAh/g (corresponding to the stoichiometric stage-one compound LiC_6), excellent cycle life when properly passivated, and low cost (Basu, 1982; Zaghib et al., 2013). Nevertheless, graphite-based anodes are increasingly approaching their practical performance limits, particularly with respect to fast-charge capability, low-temperature operation, ultimate energy density, and safety.

The thermodynamic reduction potential of graphite lies above the lowest unoccupied molecular orbital (LUMO) of standard carbonate-based electrolytes. Consequently, during the initial formation cycles, reductive decomposition of the electrolyte generates a passivating solid-electrolyte interphase (SEI) on the graphite surface. While this SEI is crucial for long-term kinetic stability by preventing continuous electrolyte reduction, it imposes several drawbacks: irreversible lithium loss, increased impedance, sluggish Li^+ diffusion at high rates or low temperatures, and a propensity for uneven lithium plating and dendritic growth – especially under aggressive charging protocols – ultimately raising the risk of internal short circuits and thermal runaway.

In contrast, the spinel lithium titanate $Li_4Ti_5O_{12}$ (LTO) exhibits a redox potential of approximately 1.55 V versus Li/Li^+, situated well within the electrochemical stability window of conventional carbonate-based electrolytes. This positioning eliminates SEI formation entirely and enables near-zero volumetric strain ($< 1\%$) upon cycling, conferring exceptional cycle life ($> 10\,000$ cycles) and intrinsic safety. However, the elevated voltage and modest theoretical capacity (175 mAh/g, practical ≈ 160 mAh/g) substantially reduce full-cell energy density, restricting LTO to specialised applications where safety and longevity supersede energy requirements (Thackeray, 1999; Yang et al., 2023).

To overcome the limitations of both graphite and LTO, intensive research is directed toward high-capacity alloying and conversion-type anode materials. Silicon, germanium, tin, antimony, phosphorus, and their oxides, carbides (e.g., SiC, or SiO_x), as well as numerous carbon-based nanocomposites, are under active investigation (Leonova et al., 2023). Among these, tin-oxide-based anodes have demonstrated encouraging performance, achieving reversible capacities in excess of 650 mAh/g at current densities up to 1000 mA/g while retaining stable cycling over at least 100 cycles (Florez Gomez et al., 2024). Similarly, antimony–titanium-oxide composite systems have delivered specific capacities of ≈ 536 mAh/g after 100 cycles at 100 mA/g, coupled with excellent rate capability across a wide range of current densities (Gomez et al., 2024). These emerging materials offer the prospect of dramatically higher gravimetric and volumetric capacities than graphite, provided that challenges related to large volume expansion (up to 300% for Si), SEI instability, and particle pulverisation can be effectively mitigated through nanostructuring, protective coatings, advanced binders, and optimised electrolyte formulations.

3.2. Cathodes for LIBs

Three principal families of intercalation compounds currently dominate as cathode materials in commercial lithium-ion batteries, i.e. layered $LiMO_2$ (where M = Co, Ni, Mn or their combinations), spinel $LiMn_2O_4$, and olivine $LiFePO_4$ (Basu, 1982; Limachi et al., 2024; Padhi et al., 1997).

Layered oxides belonging to the $R-3m$ structure (α-$NaFeO_2$-type) offer the highest practical specific capacity of the three classes, with state-of-the-art materials now routinely achieving 180–220 mAh/g in full cells. This superiority arises from their two-dimensional Li^+ diffusion pathways and the ability to extract a large fraction of lithium before the host structure becomes unstable. However, long-term stability strongly depends on both composition and state of charge. Instability manifests in two primary forms: (i) structural degradation caused by transition-metal migration from octahedral sites in the TM layer to octahedral sites in the Li layer via intermediate tetrahedral coordination, and (ii) chemical instability linked to oxygen-anion redox activity at high degrees of delithiation (Qian et al., 2022).

Among the parent ternary end-members, Co^{3+} imparts excellent structural integrity owing to its high octahedral site stabilisation energy (OSSE), yet $Li_{1-x}CoO_2$ becomes chemically unstable when $x > 0.5$ because the $Co^{3+/4+}$: t_{2g} band overlaps the top of the O^{2-} : $2p$ band, leading to partial oxidation of lattice oxygen and irreversible O_2 release (Chebiam et al., 2001; Grey et al., 2004). Batteries equipped with cobalt-based layered oxide cathodes exhibit high voltages of around 4.4 V and are common in wearable consumer technology (Li et al., 2026).

$Mn^{4+/3+}$, conversely, provides outstanding chemical stability but is prone to cation migration and layered-to-spinel transformation owing to the low OSSE of Mn^{3+} (Sangsanit et al., 2025). $Ni^{2+/3+/4+}$ occupies an intermediate position, offering reasonable structural resilience while the pronounced Ni-O covalency enhances intrinsic electronic conductivity. Cost and toxicity also follow the order Co > Ni > Mn.

To exploit the complementary strengths of the three metals, the industry has converged on compositionally balanced materials such as $LiNi_{1/3}Mn_{1/3}Co_{1/3}O_2$ (NMC-111) and, increasingly, nickel-rich variants (NMC-622, NMC-811, etc.), which provide the optimum compromise among energy density, cycle life, intrinsic safety, and raw-material considerations (Zheng et al., 2023). The above-mentioned advantages of nickel and manganese-rich electrodes made batteries incorporating them more universal than cobalt analogues, and contributed to their wider application. Manganese and nickel-containing layered oxide cathodes have been a choice not only for portable electronics but also for electric vehicles and energy storage systems (Shahid and Agelin-Chaab, 2023).

The cubic spinel $LiMn_2O_4$ ($Fd-3m$) features a robust three-dimensional interstitial network that facilitates rapid Li^+ diffusion, endowing it with excellent power capability and structural resilience without major phase transformations during cycling. Its practical capacity is restricted to < 120 mAh/g, and long-term durability is compromised by Mn dissolution triggered by disproportionation of Mn^{3+} into Mn^{4+} and soluble Mn^{2+}. This process is catalysed by trace protons originating from hydrolysis of $LiPF_6$ in the presence of residual water (typically ppm levels). Despite these limitations, the low cost and acceptable power performance of $LiMn_2O_4$ (often blended with NMC) make it attractive for certain grid-storage applications (Koech et al., 2024).

The olivine $LiFePO_4$ ($Pnma$) is distinguished by exceptional thermal stability and intrinsic safety. Strong covalent bonding within the polyanion $(PO_4)^{3-}$ units suppresses oxygen release even under severe abuse conditions. As originally elucidated by Manthiram and Goodenough (1980s), the inductive effect of the polyanion lowers the $Fe^{2+/3+}$ redox energy relative to oxides, raising the operating voltage to ≈ 3.4 V versus lithium and thereby increasing energy density compared with earlier polyanion systems. Drawbacks include modest theoretical capacity (170 mAh/g, practical < 160 mAh/g), low average voltage, poor intrinsic electronic conductivity ($\approx 10^{-9}$–10^{-10} S cm^{-1}), and one-dimensional Li^+ diffusion. These shortcomings are routinely mitigated by nanosizing the particles and applying conductive carbon coatings, although such measures further reduce an already unfavourable volumetric energy density. The olivine $LiFePO_4$ is applied in the same areas as nickel and manganese layered oxides but provides higher cyclability and is more environmentally friendly (Yuan et al., 2011).

Among the three established intercalation cathode families, layered transition-metal oxides remain unrivalled in delivering the highest gravimetric and volumetric energy density, which explains their dominance in electric-vehicle applications where driving range is paramount (Manthiram, 2017; Nandihalli et al., 2024; Nitta et al., 2015; Zanoletti et al., 2024).

4. SODIUM-ION BATTERIES (SIBS)

The development of sodium-ion batteries has started as a possible solution for environmental issues connected with lithium mining. Sodium-ion batteries can be cheaper due to greater abundance and less costly supply charges (Nekahi et al., 2024). Sodium-ion batteries also provide functional benefits such as higher power, faster charging, and low-temperature operation (Zhao et al., 2024). The downside of this technology is lower energy, which causes a higher need for storage units to supply the same amount of energy as the corresponding LIBs. Sodium is readily available in seawater, although sodium carbonate deposits represent a more practical and concentrated industrial source and occur widely across the globe. Owing to the chemical analogies between sodium and lithium, the corresponding technologies have advanced rapidly and have already entered the stage of commercial deployment. Physicochemical differences between the first two group metals, such as redox potential, are relevant for battery construction. Lower redox potential causes less energy to be delivered to the cathode compared to LIB. The higher atomic mass of sodium relative to lithium inherently results in lower gravimetric energy density, a critical drawback when evaluating the life-cycle environmental impact of a battery system (Schirber, 2024).

4.1. Anodes for SIBs

In carbon materials, intercalation of sodium occurs especially in ester-based electrolytes. Carbonaceous anode materials can be classified into graphitic carbon, expanded graphite, and amorphous carbons, with the latter category encompassing non-graphitizable hard carbon and graphitizable soft carbon. These classes of carbon exhibit distinct sodiation and desodiation behaviours, which vary according to the electrolyte system employed (Jia et al., 2024). Lately, there is also a need for the synthesis of carbon materials from natural materials, which produce amorphous carbon (Kim et al., 2023; Wu et al., 2024). Such materials exhibit larger interlayer spacing than graphite, leading to an adsorption/intercalation mechanism in ester-based electrolytes and, unfortunately, a co-intercalation mechanism in ether-based electrolytes (Wahid et al., 2018). Larger layer spacing is also present in expanded graphite and undergoes a combined adsorption-intercalation process during charge-discharge when operated in ester-based electrolyte systems (Pan et al., 2024; Wen et al., 2014). Similar ion transfer occurs in TiO_2 and Nb_2O_5 charge-discharge (Liu et al., 2018). Interestingly, 2D carbon materials such as MXenes, which are 2D metal carbides, can act as an intercalation anode with a relatively limited capacity, also thanks to the larger interlayer spacing (Jia et al., 2023; Wang et al., 2015).

Interesting material for anodes was synthesised by embedding carbon fiber with tin oxide nanopowder, with a capacity of 1275 mAh/g at 50 mA/g (Kim et al., 2021).

Another interesting mechanism occurs in anodes with elements such as Sn, Sb, Bi, Si, Ge, and P. These kinds of electrodes exhibit alloying reactions with a universal equation written as follows (Eq. (1)) (Choi et al., 2024).

$$M + nNa^+ + ne^- \rightarrow Na_nM \quad (1)$$

Alloying-type negative electrodes react with sodium through the formation of binary intermetallic compounds Na_nM (where M = Sn, Sb, Si, Ge, Bi, P, etc.). The gravimetric capacity of the mentioned materials scales with the maximum number of sodium atoms accommodated per atom of M (i.e., the electron-transfer number n), which in turn depends on the atomic mass of the host element.

Tin forms $Na_{15}Sn_4$ upon full sodiation ($n = 3.75$), delivering a theoretical specific capacity of 847 mAh/g. However, this is accompanied by a massive volumetric expansion of approximately 420% (Darwiche et al., 2012; Passerini et al., 2024). Antimony alloys to Na_3Sb ($n = 3$), providing 660 mAh/g with a similarly severe expansion of $\approx$ 390% (Darwiche et al., 2012; Passerini et al., 2024). Germanium exhibits a more modest theoretical capacity of 396 mAh/g (NaGe), while bismuth reaches 385 mAh/g via the Na_3Bi phase ($n = 3$) (Abel et al., 2013; Su et al., 2015).

Silicon, despite its outstanding performance in lithium-ion systems, reacts only partially with sodium, forming amorphous $Na_{0.76}Si$ at room temperature. This limited sodiation nevertheless yields a respectable 725 mAh/g and, crucially, a comparatively low volume expansion of only $\approx$ 114%, making silicon one of the more mechanically tolerant high-capacity hosts for sodium (Jung et al., 2014).

Red phosphorus stands out with by far the highest theoretical capacity of any known sodium-ion anode material: 2596 mAh/g, corresponding to the formation of Na_3P ($n = 3$). Both theoretical and experimentally achievable values place phosphorus at the pinnacle of gravimetric performance among sodium-ion anode candidates.

Notwithstanding their exceptional capacities, alloying anodes universally suffer from extreme volumetric strains during sodiation/desodiation (Fig. 2). Repeated expansion and contraction induce particle fracturing, pulverisation, loss of electrical contact, and continuous reformation of the solid-electrolyte interphase, all of which culminate in rapid capacity decay and poor cycle life (Ni et al., 2018; Nowak et al., 2024). Successful commercialisation, therefore, hinges on the development of effective nanostructuring, protective coatings, composite architectures, and tailored electrolyte formulations capable of accommodating or mitigating these mechanical stresses.

The practical deployment of alloying and conversion-type anodes in sodium-ion batteries is critically limited by their poor

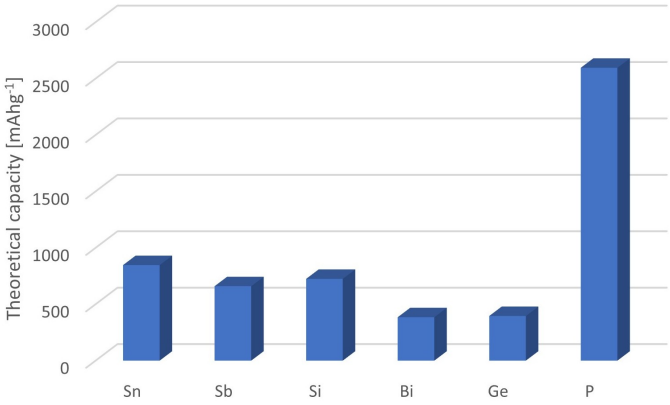

Figure 2. Theoretical capacities of sodium binary alloys vs the alloying element.

long-term stability. Substantial improvements are therefore required through deliberate nanostructural engineering, composite design, and precise control of the electrode-electrolyte interphase (Ying and Han, 2017).

A widely explored mitigation strategy involves the incorporation of conversion-type non-metallic elements (P, S, O, N, F, Se, etc.) that react reversibly with sodium to form Na_nX compounds. In practice, these elements are rarely used in pure form; instead, they are pre-combined with metallic or non-metallic hosts (both alloying and non-alloying) to yield oxides, sulphides, selenides, phosphides, nitrides, or fluorides. During the initial sodiation, these compounds undergo a displacement (conversion) reaction of the general form (2).

$$nNa^+ + ne^- + M^{n+}X \rightarrow Na_nX + M \quad (2)$$

in which the electrochemically generated metallic phase (M) subsequently serves as a conductive matrix or buffer for further alloying reactions, while the Na_nX phase contributes additional capacity.

Among conversion compounds, metal oxides, sulphides, and especially phosphides exhibit attractive specific capacities and relatively low average sodiation potentials, making them appealing candidates for high-energy sodium-ion cells. Table leg, like their pure alloying counterparts, conversion anodes suffer from pronounced volumetric changes during cycling, severe particle pulverisation, repeated fracturing and reformation of the solid-electrolyte interphase, and consequent rapid capacity fade. These interrelated degradation modes remain the principal obstacles to their commercialisation (Wei et al., 2024; Zhang et al., 2019b).

Overcoming these challenges demands multifaceted approaches, including yolk-shell or core-shell architectures, embedding active particles within porous carbon scaffolds, in situ formation of flexible buffering matrices, and the design of artificial interphases or sodium-compatible electrolyte additives that can accommodate large strain while preserving electrical continuity and ionic accessibility.

4.2. Cathodes for SIBs

Transition-metal oxides of the form Na_xMO_2 (M = Co, Mn, Fe, Ni, etc.) have gained significant attention as intercalation cathodes for sodium-ion batteries (SIBs), owing to their structural analogy with established lithium-ion counterparts. The crystallographic architecture of these oxides is highly sensitive to synthesis parameters and sodium stoichiometry, resulting in a broad spectrum of phases. Electroactive Na_xMO_2 cathodes are broadly categorised into layered and tunnel structures, both of which can be prepared via air-compatible techniques such as solid-state sintering, co-precipitation, or hydrothermal processing (Billaud et al., 2014; Delmas et al., 1980).

Layered Na_xCoO_2 has been a focal point of early research, inspired by the commercial success of $LiCoO_2$. However, the larger ionic radius of Na^+ (1.02 Å vs. 0.76 Å for Li^+) induces pronounced lattice strain, yielding suboptimal practical capacities of 70–100 mAh/g and mediocre rate capability (Kehne et al., 2019; Lei et al., 2014; Shibata et al., 2015). Phase-pure variants of Na_xCoO_2 can be selectively accessed through high-temperature solid-state methods by fine-tuning the Na:Co precursor ratio, enabling control over stacking sequences (e.g., O3, P2, P3 phases) and electrochemical properties.

In comparison, Na_xMnO_2 layered oxides offer greater promise, with a theoretical capacity of 243 mAh/g derived from the $Mn^{3+/4+}$ redox couple, alongside the economic and environmental advantages of manganese. Practical capacities in these systems span 160–219 mAh/g, yet they are plagued by structural degradation, including amorphisation and collapse under repeated Na^+ extraction/insertion, driven by Jahn-Teller distortions and cumulative lattice strain (Hidalgo et al., 2024). Layered $NaFeO_2$, leveraging abundant iron resources and the highly reversible $Fe^{4+/3+}$ couple, exhibits voltage-dependent performance. Capacities of 80–100 mAh/g are achievable when the upper cut-off is restricted to 3.4 V vs. Na/Na^+; higher voltages provoke irreversible phase transitions, loss of Na^+ diffusion pathways, and capacity fade (Zhao et al., 2013). Additional single-transition-metal oxides, such as $NaCrO_2$ (Kubota et al., 2015), $NaNiO_2$ (Han et al., 2014), and $Na_xV_yO_i$ (Dong et al., 2015), have also been evaluated as viable intercalation hosts.

Tunnel-structured Na_xMO_2 oxides adopt an orthorhombic framework, characterised by one-dimensional Na^+ diffusion channels that inherently limit rate performance compared with two- or three-dimensional counterparts (Liu et al., 2024; Sauvage et al., 2007). $Na_{0.44}MnO_2$, with its theoretical capacity of 121 mAh/g, remains the most studied tunnel cathode and can be synthesised via diverse routes, including solid-state reactions (Sauvage et al., 2007), hydrothermal treatments (Hosono et al., 2012), solution combustion (Saint et al., 2008), or sol-gel processes (Xu et al., 2014).

Notably, sol-gel-derived sub-micrometre $Na_{0.44}MnO_2$ slabs have demonstrated capacities exceeding 120 mAh/g, coupled with robust cycling stability over 100 cycles, highlighting the efficacy of morphology control in enhancing accessibility and mechanical integrity (Xu et al., 2014). Beyond oxides, polyanionic compounds represent a burgeoning class of SIB cathodes, prized for their structural versatility, thermal resilience, and elevated operating potentials arising from the inductive withdrawal of electron density by the polyanion. Prominent examples encompass phosphates (e.g., $Na_3V_2(PO_4)_3$), mixed phosphates/pyrophosphates (e.g., $Na_2FeP_2O_7$), fluorophosphates (e.g., $NaVPO_4F$), and sulphates (e.g., $NaFeSO_4F$), which collectively deliver high voltages (> 3.5 V) and exceptional cycle life, albeit often at the expense of gravimetric capacity. Polyanionic compounds can also possess other transition metals in their structure, such as manganese, nickel, cobalt, molybdenum, titanium and tungsten. Addition of nickel, manganese and titanium improves voltages and energy densities, while cobalt, molybdenum and tungsten improve structural stability of electrodes during charge/discharge cycles (Dacek et al., 2016; Xu et al., 2023). Another class of polyanionic compounds are fluorophosphates $Na_3M_2(PO_4)_2F_3$. In SIB cathodes, their derivates with iron, vanadium and vanadium oxide are of high interest. Iron derivate is mostly used for its cost-effectiveness. Vanadium derivate possesses a high capacity of around 243 mAh/g and a high voltage of around 4.1 V, vanadium oxide derivates provide additional stability for high power applications (Dacek et al., 2016; Hwang et al., 2025). Alluaudites are another class of polyanionic compounds with $Na_2Fe_2(SO_4)_3$ being an exemplary material exhibiting 3.8 V potential and 405 Wh/kg energy density (Liu and Palmore, 2017).

Prussian blue analogues – metal hexacyanometallates – constitute another promising framework family, wherein transition-metal cations are octahedrally bridged by cyanide ligands to form an open cubic lattice with spacious interstitial sites for reversible Na^+ occupancy. Early studies in aqueous electrolytes (e.g., with Ag/AgCl references) revealed commendable cycling durability and rate capability, though limited by modest discharge voltages (< 1.5 V). These constraints, attributable to the aqueous medium and reference electrode, have spurred investigations into non-aqueous SIB configurations, where hexacyanometallates such as $Na_2MnFe(CN)_6$ exhibit voltages approaching 3.5 V and capacities > 100 mAh/g (Wessells et al., 2011a).

Organic materials offer a sustainable alternative for SIB cathodes, with ongoing efforts centred on organosulphur, radical, carbonyl, and polymeric systems. Aromatic carbonyl derivatives, in particular, function via reversible Na^+ coordination to the C=O redox centre, typically at ≈ 2.2 V vs. Na/Na^+, affording capacities of 140–250 mAh/g and retention over 40–200 cycles, modulated by molecular weight and conjugation (Sakaushi et al., 2013). Pteridine-based organics and conjugated polymers further expand this palette.

Anion-insertion cathodes, predominantly polymeric or doped variants, enable operation at higher potentials (> 3.0 V) through the accommodation of large anions (e.g., PF_6^-, ClO_4^-). For instance, a poly(aniline-co-nitroaniline) copolymer (P(AN-NA)) in $NaPF_6$/EC-DEC-DMC delivers 180 mAh/g at 3.2 V, with 96% retention after 50 cycles via

reversible $[PF_6]^-$ shuttling. Poly(triphenylamine) (PTPAn) in $NaPF_6$/DME-DOL exhibits 98 mAh/g at ≈ 3.6 V, while amorphous oligopyrene (AOL) in ClO_4^-/PC achieves 121 mAh/g at 3.5 V through ClO_4^- insertion. Polypyrrole variants doped with $[Fe(CN)_6]^{4-}$ (PPy-Fe) or diphenylamine-4-sulphonate (PPy-Ds) yield 100–135 mAh/g at ≈ 3.0 V. Intriguingly, Sakaushi and co-workers demonstrated that aromatic porous honeycomb (APH) electrodes can toggle between anion-insertion (4.1–2.8 V) and cation-insertion (2.8–1.3 V) regimes, attaining a specific power of 10 W/g and energy of 500 Wh/kg (Xiang et al., 2015).

A comparative summary of electrochemical metrics for these diverse SIB cathode classes is illustrated in Fig. 3 (Iyer et al., 2024).

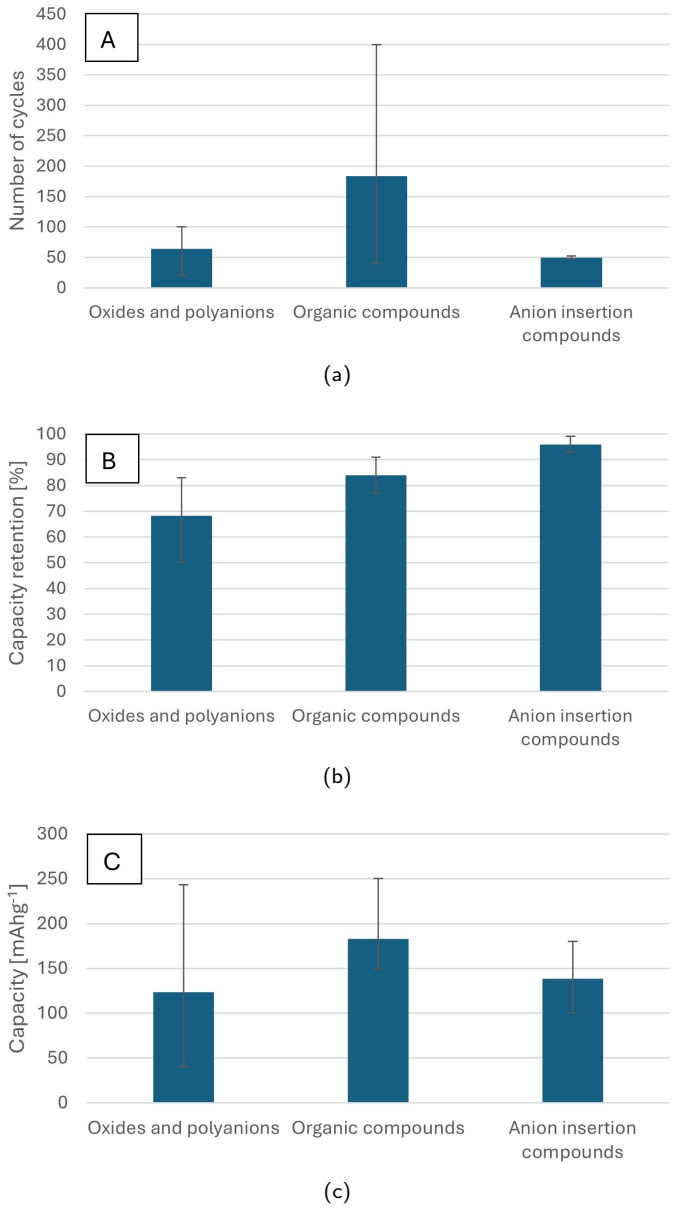

Figure 3. Performance of SIBs cathodes: (a) number of cycles, (b) capacity retention, (c) capacity.

5. POTASSIUM ION BATTERIES (KIBS)

The first functional potassium-ion battery (KIB) prototype was disclosed in 2004, employing Prussian blue as the cathode and metallic potassium as the anode. This milestone triggered a rapidly expanding body of research focused on novel electrode materials, optimised binders, and tailored electrolytes.

Potassium belongs to the same group (Group 1) of the periodic table as lithium and sodium and is far more earth-abundant than lithium (17000 ppm vs. 20 ppm in the Earth's crust), conferring a substantial raw-material cost advantage. Although metallic potassium is currently more expensive than sodium metal, the key precursor for cathode synthesis – potassium carbonate (K_2CO_3) – is priced comparably to sodium carbonate (Na_2CO_3). Consequently, assuming equivalent processing and supply-chain maturity, any mature KIB technology is projected to undercut the cost of present-day lithium-ion systems.

A distinctive electrochemical feature of KIBs is their potential for high operating voltage and energy density. In aqueous standard conditions, the K^+/K couple exhibits a redox potential of −2.936 V vs. SHE, comparable to that of Li^+/Li (−3.040 V) and considerably lower than Na^+/Na (−2.714 V) (Zhang et al., 2019a). More importantly, this trend is amplified in non-aqueous media. Solvated-ion theoretical calculations and experimental measurements in carbonate esters consistently show that the standard electrode potential of K^+/K is the most negative among alkali metals in common battery electrolytes.

In propylene carbonate (PC), for example, the computed potentials are approximately −2.79 V (Li), −2.56 V (Na), −2.88 V (K), −2.95 V (Rb), and −3.10 V (Cs) versus the respective alkali-metal reference (Anoopkumar et al., 2020).

Similar rankings hold across ethylene carbonate, dimethyl carbonate, and ether-based solvents. The anomalously low desolvation energy and weak solvation shell of K^+ in organic electrolytes are responsible for this counterintuitive behaviour, effectively positioning the K^+/K couple below Li^+/Li on the electrochemical scale under practical battery conditions.

As a direct consequence, full KIB cells can in principle deliver higher average discharge voltages than their lithium-ion counterparts when paired with identical cathode materials, translating into superior gravimetric and volumetric energy density – provided suitable high-capacity, K^+-compatible electrodes and stable electrolytes can be developed. This intrinsic thermodynamic advantage, combined with resource abundance, underpins the growing academic and industrial interest in potassium-ion batteries as a credible post-lithium technology.

Due to economic reasons, potassium is a viable material because of its abundance and even geographical distribution. Potassium ion has many advantages over sodium and lithium, but as it has a larger molecular weight, KIBs did not attract substantial interest in the early stages of research. However, when comparing two analogous systems employing Prussian

blue cathodes and carbon-based anodes, the potassium-ion configuration is only 7.85% heavier than its competing sodium-ion counterpart (Ge et al., 2022). Therefore, potassium ion batteries do not have to exhibit lower energy density than those based on lighter metals.

A further practical benefit of potassium chemistry is its negligible alloying reactivity with aluminium at potentials relevant to anode operation. Unlike lithium, which readily forms Li-Al alloys below ≈ 0.3 V vs. Li/Li^+ and therefore mandates the use of costlier copper foil as the negative-side current collector, potassium shows no thermodynamically favourable alloying with aluminium across the entire operating window of typical KIB anodes. Conclusionally, lightweight and inexpensive aluminium foil can be employed on both electrodes without risk of degradation, offering a meaningful reduction in cell-level materials cost and overall stack weight – advantages that are not similarly realised in lithium-ion technology.

The solvation behaviour of K^+ ions in non-aqueous electrolytes also confers distinct kinetic benefits. Owing to its large bare ionic radius (1.38 Å) and comparatively low charge density, K^+ exhibits the weakest Lewis acidity among the alkali-metal cations. This results in the loosest solvation sheath and the lowest cation-solvent interaction energy in common carbonate and ether solvents, as corroborated by both ab initio calculations and spectroscopic measurements. The primary solvation number for K^+ is typically 4–5, markedly lower than the 6–7 observed for Li^+ and Na^+, yielding the smallest effective solvated radius and the highest ionic mobility.

Experimental ionic conductivities of potassium-based electrolytes routinely exceed those of analogous lithium or sodium salts at equivalent concentrations, while maintaining high cation transference numbers. These attributes underpin the outstanding rate performance routinely observed in KIB prototypes, even with relatively thick electrodes and conventional separator materials.

Finally, potassium readily intercalates into graphite to form the stage-I compound KC_8, delivering a reversible specific capacity of 273 mAh/g (the theoretical value is 279 mAh/g for the reaction $8C + K^+ + e^- \rightleftharpoons KC_8$).

This capacity is substantially higher than the ≈ 35 mAh/g achievable with sodium under comparable conditions and eliminates the need for the complex hard-carbon anodes required in sodium-ion systems. The ability to utilise inexpensive, widely available graphite as a high-performance anode, coupled with aluminium current collectors and a high-voltage cathode, positions potassium-ion technology as a uniquely cost-effective and energy-dense complement to existing lithium-ion platforms (Anoopkumar et al., 2020).

5.1. Cathodes for KIBs

The inaugural potassium-ion battery prototype utilised Prussian blue (PB) as the cathode material. Since that demonstration, PB and its analogues have been the subject of intensive investigation as cathodes for KIBs (Xiang et al., 2015). Additional classes of cathode materials under active exploration include layered transition-metal oxides (Nathan et al., 2022), polyanionic compounds, and organic crystalline frameworks (Hosaka et al., 2019). Prussian blue, chemically ferric(III) hexacyanoferrate(II), $Fe_4[Fe(CN)_6]_3$, exhibits an open-framework structure that enables highly reversible K^+ intercalation. Studies have shown that PB thin films can withstand millions of potassiation/depotassiation cycles with negligible structural deterioration and minimal capacity loss.

Analysis of electrochemical tests leads to the assessment that K^+ ions are intercalating in PB crystals. The reactions that occur on Prussian blue films are the oxidation of Prussian blue to Berlin green and its reduction to Prussian white.

Early studies on KIB cathodes focused on K_xCoO_2-type layered potassium metal oxide, which gave specific capacities of around 60 mAh/g at voltages in the range of 2–3.9 V. A further advance toward high-capacity materials has led to the development of iron- and manganese-based potassium oxide cathodes. The studied compounds delivered reversible capacities of 136–178 mAh/g with cycle life extending to 200 cycles. Regrettably, their average discharge potentials are notably lower than those of the corresponding sodium-based analogues (Nathan et al., 2022).

Manganese-based cathode systems tend to exhibit low cost and non-toxicity. However, the presence of Mn^{3+} ions can adversely influence the electrochemical performance of these materials. In other research, it was shown that this can be decreased through metal doping methods. The drawback of these cathodes is vulnerability towards water intercalation and oxidation. This leads to the need for the use of inert gases during cell assembly (Jian et al., 2015).

5.2. Anode materials for KIBs

Carbon-based materials, predominantly graphite, are widely employed as negative electrodes in alkali-metal-ion batteries. Theoretical investigations have established that K^+ intercalation into graphite is thermodynamically more favourable than that of other alkali-metal cations (Chen et al., 2019). The primary challenge hindering KIB development remains the identification of a robust anode capable of reversibly hosting the large K^+ ion over repeated insertion/extraction cycles without significant structural degradation. In parallel with trends observed in sodium-ion systems, considerable effort is currently devoted to deriving carbon anodes from abundant natural precursors (Ma et al., 2024).

Potassium graphite complexes can be obtained by pyrolysis of a potassium metal and graphite mixture. Research has demonstrated that potassium ions intercalate into graphite by occupying the interlayer galleries, leading to graphite expansion and exfoliation (Li et al., 2019). Other studies were performed on non-graphitic carbon nanofibers (CNF). However,

low-capacity retention was observed with a 73% reduction after 20 cycles. It was suggested that disordered carbon can hold a larger number of ions smaller layer expansion during intercalation (Li et al., 2024). Researchers released a paper showing that potassium ions (K^+) can be reversibly inserted into and extracted from a graphite electrode using a non-aqueous electrolyte, achieving a reversible capacity of 273 mAh/g. The addition of low-density soft carbon was shown to enhance both cycle life and rate performance (Komaba et al., 2015). In separate work, scientists developed a hollow carbon material derived from melamine-formaldehyde resin, which was transformed through pyrolysis into a neuron-inspired architecture and tested as an anode for potassium-ion batteries. Thanks to its inherent structural flexibility and good electrical conductivity, this material could serve directly as the anode without requiring a current collector, binder, or conductive additives. The nanostructured electrode delivered a reversible capacity of 340 mAh/g at 0.1 C, outstanding cycling stability with nearly full capacity retention ($\approx$ 100%) after 150 cycles at 0.5 C, and high Coulombic efficiency (72.1% in the initial cycle and exceeding 99% in subsequent cycles) (Wang et al., 2018a). Commercial hard carbon, Carbotron P(J) supplied by Kureha Co., exhibited a reversible specific capacity of approximately 215 mAh/g while displaying exceptionally low sensitivity to air and moisture – an essential characteristic for the practical deployment of potassium-ion batteries (Kubota et al., 2018). Among non-carbon intercalation hosts, molybdenum disulfide (MoS_2), a representative transition-metal dichalcogenide (TMD), has attracted considerable interest as a KIB anode owing to its natural abundance, low cost, and layered crystal structure that provides two-dimensional diffusion pathways for K^+ ions. Nevertheless, the intrinsic poor electronic conductivity of MoS_2 continues to restrict its rate capability and long-term electrochemical stability (Wang et al., 2024).

6. MAGNESIUM BATTERIES (RMBS)

Rechargeable magnesium batteries (RMBs) employ metallic magnesium as the negative electrode, which offers a high volumetric capacity of 3833 mAh/cm^3 (Mousavian and Bautin, 2025) and a markedly reduced propensity for dendrite formation compared with alkali metals. The low standard redox potential of the Mg^{2+}/Mg couple (−2.37 V vs. SHE) (Atkins et al., 2017) combined with its divalent charge carrier, it promises substantially higher theoretical energy densities than monovalent systems. Nevertheless, established design principles and materials developed for alkali-metal batteries cannot be directly transferred to magnesium chemistries owing to fundamental differences in ion solvation, interfacial passivation behaviour, and electrolyte compatibility.

6.1. Cathodes for RMBs

In contrast to monovalent alkali-metal systems, rechargeable magnesium batteries suffer from a scarcity of suitable high-capacity intercalation cathodes capable of reversibly hosting the divalent Mg^{2+} ion.

Particle nanosizing remains a proven strategy to minimise solid-state diffusion limitations by reducing ion-transport path lengths and increasing reactive surface area (Mao et al., 2020). For instance, non-stoichiometric anatase TiO_2 deliberately engineered with titanium vacancies via fluorine doping has been shown to enhance Mg^{2+} diffusion kinetics and provide additional charge-storage sites (Levi et al., 2008).

A noteworthy advance is the demonstration of dual-cation co-intercalation in the Chevrel phase Mo_6S_8 using Mg-Li hybrid electrolytes, whereby both Li^+ and Mg^{2+} contribute to charge compensation and enable dendrite-free magnesium deposition. Although highly effective in Mo_6S_8, this co-intercalation approach has only rarely been extended to other host lattices (Richard et al., 2017).

Transition-metal oxides are widely investigated as RMB cathodes because their strong metal-oxygen bonds confer high redox potentials and reasonable oxidative stability. Prominent candidates include V_2O_5, MnO_2, MoO_3, and various TiO_2 polymorphs (Masese and Kanyolo, 2023).

Layered α-V_2O_5 permits room-temperature Mg^{2+} insertion accompanied by a phase transition to δ-$Mg_xV_2O_5$; the expanded interlayer gallery in the δ-phase facilitates faster Mg^{2+} mobility and yields a higher operating voltage. Performance is further improved by particle downsizing, structural or electrolytic water incorporation, pillar pre-intercalation, expanded interlayer spacing, and carbon compositing. Bilayered V_2O_5 nanoribbons supported on carbon nanofoam, for example, achieved an initial discharge capacity of 240 mAh/g, albeit with rapid subsequent fading (Tepavcevic et al., 2015; Zhang et al., 2023b).

Orthorhombic α-MoO_3 is another attractive intercalation host, but structural rearrangements during cycling typically cause steep capacity decay. Nanostructured α-MoO_3 electrodes have delivered $\approx$ 220 mAh/g at $\sim$ 1.8 V vs. Mg/Mg^{2+}. Mild fluorination to form $MoO_{2.8}F_{0.2}$ lowers lattice energy, boosts electronic conductivity, markedly accelerates Mg^{2+} diffusion, and improves cycling stability (Gershinsky et al., 2013; Wan et al., 2016).

Polymorphic TiO_2, particularly anatase and TiO_2(B), also functions as an RMB cathode, although strong electrostatic Mg^{2+}–lattice interactions severely hamper reversible insertion. Defect engineering, especially fluorine doping, generates active intercalation sites and significantly enhances performance. Optimised F-doped TiO_2 electrodes have demonstrated reversible capacities of $\sim$ 150 mAh/g with excellent retention over 300 cycles at 300 mA/g (Koketsu et al., 2017).

MnO_2 stands out as a very attractive cathode material thanks to its straightforward preparation, rich variety of crystal structures, and the ease with which its electrochemical properties can be adjusted. Nano-sized α-MnO_2 featuring the

(2 × 2) tunnel structure delivered an impressive initial discharge capacity of approximately 280 mAh/g. Nevertheless, the material suffered from fast capacity fading in the following cycles. Investigation of the Mg^{2+} insertion process in α-MnO_2 suggests a progressive transformation to MnO occurring at the surface/interface, ultimately leading to the creation of a K-αMnO_2@(Mg,Mn)O core-shell structure after complete discharge. Birnessite-type MnO_2, when cycled in water-containing magnesium electrolytes, delivers a high discharge capacity of 227.6 mAh/g at an average potential of 2.8 V vs. Mg^{2+}/Mg, primarily through a reversible Mg^{2+} intercalation mechanism. In contrast, the same material in conventional non-aqueous electrolytes undergoes a conversion-type reaction pathway, as reported by Sun and co-workers (Sun et al., 2016; Tolstoy et al., 2019). Both nanosizing the primary particles and expanding the interlayer gallery have been confirmed as powerful strategies for enhancing rate capability and reversible capacity in MnO_2-based cathodes (Koketsu et al., 2017). A comparison of the specific capacities achieved with various oxide cathodes in rechargeable magnesium batteries is shown in Fig. 4.

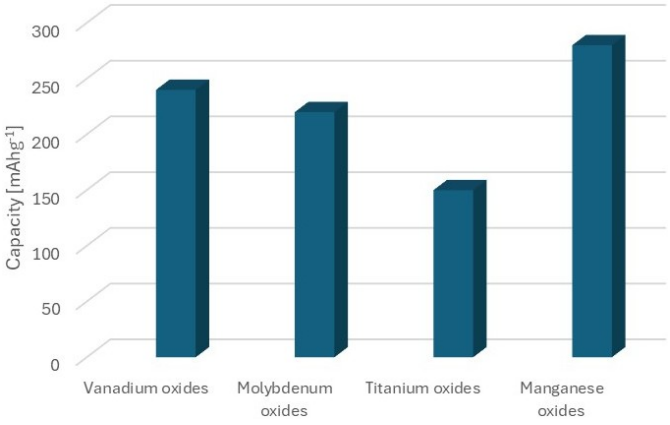

Figure 4. Capacities of metal oxide cathodes for RMBs.

6.2. Anode materials for RMBs

The relatively low reactivity of magnesium metal permits its direct use as a negative electrode in RMBs. Mg electrodeposition typically produces smooth, uniform layers and exhibits a markedly lower dendrite propensity than alkali metals, conferring intrinsic safety – though dendrite-free plating is not guaranteed under all electrolyte conditions. However, in conventional polar aprotic electrolytes, the Mg surface rapidly develops an ionically blocking passivation film, prompting intense research into three main anode strategies: surface-modified Mg metal, low-potential intercalation hosts, and alloying/conversion-type materials (Ling and Zhang, 2017).

Intercalation-type anodes compatible with standard Mg^{2+}-conducting electrolytes avoid passivation issues but suffer from sluggish Mg^{2+} diffusion, large volume changes, and particle fragmentation. Theoretical studies predict that defective graphene (e.g., 25% divacancy concentration) could achieve capacities up to 1042 mAh/g, while nanostructured carbons (nanotubes, nanocones, nanosheets, C_{60} cages) also show promise (Bella et al., 2021). Experimentally, graphite delivers ≈ 180 mAh/g in conventional electrolytes. Spinel $Li_4Ti_5O_{12}$ exhibits strongly size-dependent Mg^{2+} insertion, with 7–8 nm particles yielding 175 mAh/g and excellent stability (> 500 cycles). $Na_2Ti_6O_{13}$ and hollow Li_3VO_4/carbon spheres provide 166–318 mAh/g with enhanced structural robustness (Luo et al., 2020). Ultrathin TiO_2-B nanowires expose highly reactive (110) facets, enabling surface-dominated Mg^{2+} coordination and delivering 110 mAh/g with only 0.08% capacity loss per cycle (Zeng et al., 2017).

Alloying anodes offers far higher theoretical capacities and operates at low potentials. Bismuth (385 mAh/g, ≈ 0.23/0.32 V vs. Mg^{2+}/Mg), $Bi_{0.88}Sb_{0.12}$ (Wang et al., 2018b; Niu et al., 2020), Bi nanotubes (350 mAh/g, 92% retention after 200 cycles) (Shao et al., 2014), and BiOF nanosheets (335 mAh/g via in situ conversion to 2D Bi) (Tan et al., 2018) demonstrate excellent reversibility and rate performance. Tin (903 mAh/g, ≈ 0.15/0.20 V) and Sn-Sb nanoparticulate alloys reach 420 mAh/g with good rate capability and 74% retention after 200 cycles (Cheng et al., 2015). Bi-Sn alloys outperform their pure constituents owing to accelerated Mg^{2+} transport along phase boundaries and self-supporting nanoporous architectures. A breakthrough Ga-based liquid-solid interconversion anode ($Mg_2Ga_5 \leftrightarrow Ga$) recently achieved > 1000 cycles at 922.5 mA/g, marking a milestone toward practical high-power RMB anodes (Wang et al., 2019).

Although intercalation anodes eliminate passivation and enable conventional high-voltage electrolytes, the strong Mg^{2+}–host electrostatic interaction results in sluggish kinetics, elevated operating potentials, and reduced full-cell energy density compared with Mg-metal configurations. Alloying and conversion systems currently offer the most attractive combination of capacity, voltage, and cycle life for next-generation rechargeable magnesium batteries.

7. CALCIUM ION BATTERIES

Calcium ranks as the fifth most abundant element within the Earth's crust. It is also nontoxic, which allows for cleaner, more ecologically friendly products. Calcium ions also exhibit favourable electrochemical properties, showing only slightly lower deposition potential than that of lithium and higher than that of magnesium (Yin et al., 2025). The size of calcium ions is similar to that of sodium but larger than magnesium and lithium. Reversible electrochemical processes of calcium cations in electrolytes were first presented in 2016 (Ponrouch et al., 2016). Because of that fact, the research on calcium-ion batteries remains in its infancy. Currently, no working prototypes exist, and available data are of experimental and laboratory nature.

7.1. Cathode materials for CIBs

Various types of materials are investigated as cathodes for calcium-ion batteries.

The first type is polyanionic compounds based on transition metal oxide and a tetrahedral anion. Transition metal oxides include iron and vanadium. The iron polyanionic cathodes have reached a capacity of 80 mAh/g, for vanadium 88–103 mAh/g. The stability of such materials reached 400 cycles for iron polyanionic cathodes, and vanadium materials show capacity retention after 200 cycles.

Another class of cathode materials comprises organic compounds, including conducting polymers, organosulfur compounds, and carbonyl-based materials, which are distinguished by their low cost, wide availability, and environmental compatibility. These materials can be categorised into three primary groups: n-type (cations storage), p-type (anions storage), and bipolar-type (capable of storing both cations and anions). The capacity of organic compounds cathodes is between 100 and 150 mAh/g, but their capacity retention is between 50 and 79% after 5000 cycles.

Another kind of cathode materials studied for CIBs applications are metal oxides of special consideration, such as vanadium, molybdenum, manganese, and cobalt oxides.

Vanadium-based oxides include a series of compounds due to their many oxidation levels. They are of low-cost due to high abundance in the Earth's crust, and intercalation reactions between calcium cations were investigated from 2003. Several forms of V_2O_5 were investigated, both crystalline and amorphous. Research indicated that amorphous materials exhibited larger amounts of calcium cation reactions (Wu et al., 2021; Zhou et al., 2021). In recent years vanadium oxides mixed with active metals or ammonia were developed as a new kind of cathodes for CIBs. One of such popular options is calcium vanadium oxides hydrates (Jeon et al., 2022; Wang et al., 2022). Calcium modified oxides can deliver reversible capacity after 200 cycles of magnitude 141 mAh/g. In a similar fashion, magnesium-modified vanadium oxides were synthesised (Xu et al., 2019). Capacity retention 1 reached 86.9% after 500 cycles with columbic efficiency of over 98.4%. Electrochemical experiments demonstrated that the structure changed only slightly with the insertion/extraction of calcium ions. Mixed magnesium ions were stable in the interlayer during electrochemical reactions. Another element that is present in vanadium oxide cathodes is iron.

Prussian Blue Analogues (PBAs): These three-dimensional open-framework structures are considered potential candidates for calcium-ion storage due to their ability to facilitate rapid Ca^{2+} diffusion, though their low conductivity can limit performance. Similar to potassium and sodium ions, Prussian blue is used as a cathode material. Cui's group (Wang et al., 2013) demonstrated the reversible insertion of calcium ions into nickel hexacyanoferrate. Cycling voltages ranged between 0.22 and 0.92 V, and capacity retention after 2000 cycles was 53% (Wessells et al., 2011b; Mu et al., 2022). Another Prussian blue analogue that was reported was barium hexacyanoferrate. This material was used to build a working battery with a coulumbic efficiency of 90%, and a capacity of 70 mAh/g. The capacity retention of this cathode was 93% after 2000 cycles. Due to high potentials versus silver chloride copper hexacyanoferrate electrode was used. The electrochemical reaction of Ca^{2+} ion insertion is coupled with iron cation change of charge. The cathode retained much of its structural stability during cycling, resulting in 88% of capacity retention after 2000 cycles. The capacity of this copper-based Prussian blue analogue cathode was 65 mAh/g (Gheytani et al., 2017). In non-aqueous solutions, manganese-based Prussian blue analogues can be used. Lipson et al. (2015) performed research on this subject and reported a capacity of intercalation in the range of 80 mAh/g. The mechanism of insertion was investigated at 60 °C. It was assumed that high temperatures and ionic solvents accelerated the calcium ion exchange process.

7.2. Anode materials for CIBs

Anode materials for calcium-ion batteries include calcium metal, carbon-based materials (like graphite and silicon carbide), organic compounds (such as anthracene and pentacene), and metal alloys (including alloys of silicon, tin, and antimony. The most important point of investigation is their potential to store and release calcium ions reversibly. Research focuses on the improvement of their capacity, cycle life, and overall performance (Guo et al., 2025; Maltsev et al., 2024; Zhang and Guo, 2025).

The simplest approach is to use calcium metal as an anode. The benefit is achieving high current densities, but such electrodes decompose quickly during the process and give only satisfactory performances. Another problem is the dendrite growth of calcium metal.

Another investigated anode material is graphite, which has the benefit of not forming a protective insoluble layer around the electrode. The capacities reached are between 60–80 mAh/g, being stable for 500 cycles.

Another group of materials are organic compounds. Polyaromatic hydrocarbons (PAHs), including anthracene and pentacene, have emerged as promising anode materials for rechargeable batteries. They are considered prototypical carbonaceous materials. Calcium intercalants are inserted between crystalline structures bonded by van der Waals forces. Research has shown that such anodes can reach capacities up to 1000 mAh/g.

Metal alloys anodes that have been investigated are Zn, Li, Na, Al, and Si. Except for Na, they can mix with calcium and form intermetallic compositions. Examples of the alloy anodes

are Ca_3Zn, Ca_2Sn, and $CaLi_2$. These materials exhibit theoretical capacities of 1366, 903, and 3860 mAh/g, respectively (Tinker et al., 2023).

8. CONCLUSIONS

All energy storage systems presented in this article are perspectives for future applications in electrical energy grids and electric vehicles. The main argument for the development of sodium, potassium and magnesium systems is their higher abundance in Earth's crust, which is significantly higher than that of lithium. Every system faces its challenges. In the case of sodium and potassium batteries, these are safety and full temperature adaptability (Bai et al., 2024).

SIBs are considered frontrunners for addressing the demands of the grid storage market (Hirsh et al., 2020). Key challenges impeding their commercialisation include the optimisation of electrolyte composition, anode performance, stability at the electrode-electrolyte interface, safety concerns, and sustainable recyclability. These issues have been analysed in detail, alongside potential strategies for their mitigation (Zhao et al., 2023). Potassium-ion batteries (KIBs) hold considerable promise as a scalable solution for grid-level energy storage. This optimism stems from the low cost of potassium precursors and auxiliary components, which contrasts sharply with the escalating prices of lithium-based materials. Moreover, the established manufacturing infrastructure, electrode architectures, and electrolyte formulations from mature lithium-ion technology provide a robust foundation for accelerating KIB research, prototyping, and eventual commercial deployment (He et al., 2024). Magnesium batteries are still in their beginning stage (Shah et al., 2021). The construction of the prototype is challenged by various factors like diffusion kinetics and the formation of passive layers (Medina et al., 2021). However, there is a large drive to improve those drawbacks in the scientific community, and more innovative materials are being developed.

Calcium-ion batteries are still being investigated for most effective processes and electrode materials. Lithium is still being investigated, especially to make it more recyclable. There is a growing interest in recovering as many materials as possible (Fan et al., 2020; Roy et al., 2024). Contemporary lithium-ion batteries are well-suited to high-value applications such as frequency regulation, short-duration storage, and microgrids. However, their high cost and long-term concerns over the availability of critical minerals (lithium, cobalt, nickel) continue to restrict their widespread deployment for large-scale, long-duration grid storage. Among the numerous emerging alternatives, sodium-ion and potassium-ion chemistries currently represent the most actively developed and promising post-lithium options (Grey and Hall, 2020).

REFERENCES

Wang S., Quan W., Zhu Z., Yang Y., Liu Q., Ren Y., Zhang X., Xu R., Hong Y., Zhang Z., Amine K., Tang Z., Lu J., Li J., 2017. Lithium titanate hydrates with superfast and stable cycling in lithium ion batteries. *Nat. Commun.*, 8, 627. DOI: 10.1038/s41467-017-00574-9.

Abbas S.M., Fayed M.G., El-Tawil R.S., Mohamed S.G., Abdel-Ghany A.E., Hashem A.M., Mauger A., Julien C.M., 2024. Lithium-rich spinel cathode with higher energy density for sustainable Li-ion batteries operating in extended potential range. *Intell. Sustainable Manuf.*, 1, 10014. DOI: 10.70322/ism.2024.10014.

Abel P.R., Lin Y.-M., de Souza T., Chou C.-Y., Gupta A., Goodenough J.B., Hwang G.S., Heller A., Mullins C.B., 2013. Nanocolumnar germanium thin films as a high-rate sodium-ion battery anode material. *J. Phys. Chem. C*, 117, 18885–18890. DOI: 10.1021/jp407322k.

Ahangari M., Szalai B., Lujan J., Zhou M., Luo H., 2024. Advancements and challenges in high-capacity Ni-rich cathode materials for lithium-ion batteries. *Materials*, 17, 801. DOI: 10.3390/ma17040801.

Amarapala V., Darwish A.S.K., Farrell P., 2023. Storage of wind power energy: main facts and feasibility – hydrogen as an option. *Renewable Energy Environ. Sustainability*, 8, 16. DOI: 10.1051/rees/2023013.

Anoopkumar V., John B., Mercy T.D., 2020. Potassium-ion batteries: Key to future large-scale energy storage? *ACS Appl. Energy Mater.*, 3, 9478–9492. DOI: 10.1021/acsaem.0c01574.

Atkins P., de Paula J., Keeler J., 2017. Atkins' Physical Chemistry. 11th edition. Oxford University Press, Oxford.

Bai Z., Yao Q., Wang M., Meng W., Dou S., Liu H.K., Wang N., 2024. Low-temperature sodium-ion batteries: challenges and progress. *Adv. Energy Mater.*, 14, 2303788. DOI: 10.1002/aenm.202303788.

Barsegyan A.A., Baghdasaryan I.R., 2022. Prospects for the use of energy storage devices in the process of solar energy production. *Polityka Energetyczna – Energy Policy J.*, 25, 135–148. DOI: 10.33223/EPJ/155789.

Basu S., 1982. *Ambient temperature rechargeable battery*. US Patent, US4423125A.

Bella F., De Luca S., Fagiolari L., Versaci D., Amici J., Francia C., Bodoardo S., 2021. An overview on anodes for magnesium batteries: challenges towards a promising storage solution for renewables. *Nanomaterials*, 11, 810. DOI: 10.3390/nano11030810.

Besenhard J.O., Eichinger G., 1976. High energy density lithium cells: Part I. Electrolytes and anodes. *J. Electroanal. Chem. Interfacial Electrochem.*, 68, 1–18. DOI: 10.1016/S0022-0728(76)80298-7.

Billaud J., Clément R.J., Armstrong A.R., Canales-Vázquez J., Rozier P., Grey C.P., Bruce P.G., 2014. β-$NaMnO_2$: a high-performance cathode for sodium-ion batteries. *J. Am. Chem. Soc.*, 136, 17243–17248. DOI: 10.1021/ja509704t.

Bustos R., Gadsden S.A., Al-Shabi M., Mahmud S., 2023. Lithium-ion battery health estimation using an adaptive dual interacting model algorithm for electric vehicles. *Appl. Sci.*, 13, 1132. DOI: 10.3390/app13021132.

Chebiam R.V., Prado F., Manthiram A., 2001. Structural instability of delithiated $Li_{1-x}Ni_{1-y}Co_yO_2$ cathodes. *J. Electrochem. Soc.*, 148, A49. DOI: 10.1149/1.1339029.

Chen M., Wang E., Liu Q., Guo X., Chen W., Chou S.-L., Dou S.-X., 2019. Recent progress on iron- and manganese-based anodes for sodium-ion and potassium-ion batteries. *Energy Storage Mater.*, 163–178. DOI: 10.1016/j.ensm.2019.03.030.

Cheng Y., Shao Y., Parent L.R., Sushko M.L., Li G., Sushko P.V., Browning N.D., Wang C., Liu J., 2015. Interface promoted reversible Mg insertion in nanostructured tin-antimony alloys. *Adv. Mater.*, 27, 6598–6605. DOI: 10.1002/adma.201502378.

Choi I., Ha S., Kim K.-H., 2024. Review and recent advances in metal compounds as potential high-performance anodes for sodium ion batteries. *Energies*, 17, 2646. DOI: 10.3390/en17112646.

Dacek S.T., Richards W.D., Kitchaev D.A., Ceder G., 2016. Structure and dynamics of fluorophosphate Na-ion battery cathodes. *Chem. Mater.*, 28, 5450–5460. DOI: 10.1021/acs.chemmater.6b01989.

Darwiche A., Marino C., Sougrati M.T., Fraisse B., Stievano L., Monconduit L., 2012. Better cycling performances of bulk Sb in Na-ion batteries compared to Li-ion systems: an unexpected electrochemical mechanism. *J. Am. Chem. Soc.*, 134, 20805–20811. DOI: 10.1021/ja310347x.

Delmas C., Fouassier C., Hagenmuller P., 1980. Structural classification and properties of the layered oxides. *Physica B+C*, 99, 81–85. DOI: 10.1016/0378-4363(80)90214-4.

Dong Y., Li S., Zhao K., Han C., Chen W., Wang B., Wang L., Xu B., Wei Q., Zhang L., Xu X., Mai L., 2015. Hierarchical zigzag $Na_{1.25}V_3O_8$ nanowires with topotactically encoded superior performance for sodium-ion battery cathodes. *Energy Environ. Sci.*, 8, 1267–1275. DOI: 10.1039/c5ee00036j.

Fan E., Li L., Wang Z., Lin J., Huang Y., Yao Y., Chen R., Wu F., 2020. Sustainable recycling technology for Li-ion batteries and beyond: challenges and future prospects. *Chem. Rev.*, 120, 7020–7063. DOI: 10.1021/acs.chemrev.9b00535.

Florez Gomez J.F., Domenech F.C., Chang S., Dorvilien V., Oli N., Weiner B.R., Morell G., Wu X., 2024. Enhancing tin dioxide anode performance by narrowing the potential range and optimizing electrolytes. *Batteries*, 10, 334. DOI: 10.3390/batteries10090334.

Frith J.T., Lacey M.J., Ulissi U., 2023. A non-academic perspective on the future of lithium-based batteries. *Nat. Commun.*, 14, 420. DOI: 10.1038/s41467-023-35933-2.

Ge J., Fan L., Rao A.M., Zhou J., Lu B., 2022. Surface-substituted Prussian blue analogue cathode for sustainable potassium-ion batteries. *Nat. Sustainability*, 5, 225–234. DOI: 10.1038/s41893-021-00810-7.

Gershinsky G., Yoo H.D., Gofer Y., Aurbach D., 2013. Electrochemical and spectroscopic analysis of Mg^{2+} intercalation into thin film electrodes of layered oxides: V_2O_5 and MoO_3. *Langmuir*, 29, 10964–10972. DOI: 10.1021/la402391f.

Gheytani S., Liang Y., Jing Y., Dong H., Chi X., Yao Y., 2017. An Aqueous Ca-Ion Battery. *Adv. Sci.*, 4, 1700465. DOI: 10.1002/ADVS.201700465.

Godshall N.A., Raistrick I.D., Huggins R.A., 1980. Thermodynamic investigations of ternary lithium-transition metal-oxygen cathode materials. *Mater. Res. Bull.*, 15, 561–570. DOI: 10.1016/0025-5408(80)90135-X.

Gomez K., Fletes E., Parsons J.G., Alcoutlabi M., 2024. The effect of TiO_2 on the electrochemical performance of Sb_2O_3 anodes for Li-ion batteries. *Appl. Sci.*, 14, 6598. DOI: 10.3390/app14156598.

Grey C.P., Hall D.S., 2020. Prospects for lithium-ion batteries and beyond – a 2030 vision. *Nat. Commun.*, 11, 6279. DOI: 10.1038/s41467-020-19991-4.

Grey C.P., Yoon W.-S., Reed J., Ceder G., 2004. Electrochemical activity of Li in the transition-metal sites of O3 $Li[Li_{(1-2x)/3}Mn_{(2-x)/3}Ni_x]$ O_2. *Electrochem. Solid-State Lett.*, 7, A290. DOI: 10.1149/1.1783113.

Guo Y., Wang C., Tan C., Zhang D., 2025. A comprehensive review of anode materials in rechargeable calcium-ion batteries. *Chem. Eur. J.*, 31, e202500071. DOI: 10.1002/CHEM.202500071.

Han M.H., Gonzalo E., Casas-Cabanas M., Rojo T., 2014. Structural evolution and electrochemistry of monoclinic $NaNiO_2$ upon the first cycling process. *J. Power Sources*, 258, 266–271. DOI: 10.1016/j.jpowsour.2014.02.048.

Hasan M.M., Hossain S., Mofijur M., Kabir Z., Badrudd I.A., Yunus Khan T.M., Jassim E., 2023. Harnessing solar power: a review of photovoltaic innovations, solar thermal systems, and the dawn of energy storage solutions. *Energies*, 16, 6456. DOI: 10.3390/en16186456.

Hassan Q., Abbas M.K., Tabar V.S., Tohidi S., Sameen A.Z., Salman H.M., 2024. Techno-economic assessment of battery storage with photovoltaics for maximum self-consumption. *Energy Harvesting Syst.*, 11, 1–15. DOI: 10.1515/ehs-2022-0050.

Haynes W.M., Lide D.R., Bruno T.J. (Eds.), 2016. *CRC Handbook of Chemistry and Physics*. 97th edition, CRC Press.

He X., Iqbal N., Ghani U., Li T., 2024. Potassium ion batteries: recent advancements in anodic, cathodic, and electrolytic materials. *J. Alloys Compd.*, 981, 173680. DOI: 10.1016/j.jallcom.2024.173680.

Hidalgo M.Á., Lavela P., Tirado J.L., Aranda M., 2024. Modification of layered cathodes of sodium-ion batteries with conducting polymers. *Batteries*, 10, 93. DOI: 10.3390/batteries10030093.

Hirsh H.S., Li Y., Tan D.H.S., Zhang M., Zhao E., Meng Y.S., 2020. Sodium-ion batteries paving the way for grid energy storage. *Adv. Energy Mater.*, 10, 2001274. DOI: 10.1002/aenm.202001274.

Hong S., Lee H., Yu Y.-S., Park J., Kim C., 2023. Development of a rock-salt structure for high energy density lithium-ion batteries. *Electron. Mater. Lett.*, 19, 359–366. DOI: 10.1007/s13391-022-00397-x.

Hosaka T., Shimamura T., Kubota K., Komaba S., 2019. Polyanionic compounds for potassium-ion batteries. *Chem. Rec.*, 19, 735–745. DOI: 10.1002/tcr.201800143.

Hosono E., Saito T., Hoshino J., Okubo M., Saito Y., Nishio-Hamane D., Kudo T., Zhou H., 2012. High power Na-ion rechargeable battery with single-crystalline $Na_{0.44}MnO_2$ nanowire electrode. *J. Power Sources*, 217, 43–46. DOI: 10.1016/j.jpowsour.2012.05.100.

Hu C., Geng M., Yang H., Fan M., Sun Z., Yu R., Wei B., 2024. A review of capacity fade mechanism and promotion strategies for lithium iron phosphate batteries. *Coatings*, 14, 832. DOI: 10.3390/coatings14070832.

Hu J.-P., Sheng H., Deng Q., Ma Q., Liu J., Wu X.-W., Liu J.-J., Wu Y.-P., 2020. High-rate layered cathode of lithium-ion batteries through regulating three-dimensional agglomerated structure. *Energies*, 13, 1602. DOI: 10.3390/en13071602.

Huang Y.-R., Lee C.-H., Popuri S.R., Lee L.-C., 2025. Optimization of hydrometallurgical recovery of lithium, aluminum, iron, and copper from lithium-iron batteries. *Arch. Environ. Prot.*, 51, 75–82. DOI: 10.24425/AEP.2025.153751.

Hwang M., Kim R., Hwang J., Jang G., Kim W.I, Min W., Kwon D., Kim D., Park H.S., 2025. Modulating chemical state of cation site for fast and reversible Na ion storage of fluorophosphate cathodes. *ACS Energy Lett.*, 10, 6297–6306. DOI: 10.1021/acsenergylett.5c02540.

IEA, 2022. Global EV Outlook 2022 – Analysis. International Energy Agency. Available at: https://www.iea.org/reports/global-ev-outlook-2022.

IRENA, 2017. *Electricity storage and renewables: Costs and markets to 2030*. International Renewable Energy Agency, Abu Dhabi. Available at: https://www.irena.org/-/media/Files/IRENA/Agency/Publication/2017/Oct/IRENA_Electricity_Storage_Costs_2017.pdf.

Iyer V., Petersen J., Geier S., Wierach P., 2024. Design and characterization of poly(ethylene oxide)-based multifunctional composites with succinonitrile fillers for ambient-temperature structural sodium-ion batteries. *Polymers*, 16, 2806. DOI: 10.3390/polym16192806.

Jeon B., Kwak H.H., Hong S.-T., 2022. Bilayered $Ca_{0.28}V_2O_5{\cdot}H_2O$: high-capacity cathode material for rechargeable Ca-ion batteries and its charge storage mechanism. *Chem. Mater.*, 34, 1491–1498. DOI: 10.1021/ACS.CHEMMATER.1C02774.

Jeon Y., Lee D.J., Zheng H., Behara S.S., Lee J-P., Wu J., Li F., Tang W., Zhang L., Chen Y.-T., Xu D., Kim J., Song M.-S., der Ven A.V., He K., Chen Z., 2025. Lithium diffusion-controlled Li-Al alloy negative electrode for all-solid-state battery. *Nat. Commun.*, 16, 9629. DOI: 10.1038/s41467-025-64386-y.

Jia M., Zhang L., Yuan Q., 2023. Application of new COF materials in secondary battery anode materials. *Molecules*, 28, 5953. DOI: 10.3390/molecules28165953.

Jia Q., Li Z., Ruan H., Luo D., Wang J., Ding Z., Chen L., 2024. A review of carbon anode materials for sodium-ion batteries: key materials, sodium-storage mechanisms, applications, and large-scale design principles. *Molecules*, 29, 4331. DOI: 10.3390/molecules29184331.

Jian Z., Luo W., Ji X., 2015. Carbon electrodes for K-ion batteries. *J. Am. Chem. Soc.*, 137, 11566–11569. DOI: 10.1021/jacs.5b06809.

Jiang Y., Li K., Alhassan S.I., Cao Y., Deng H., Tan S. Wang H., Tang C., Chai L., 2023. Spinel $LiMn_2O_4$ as a capacitive deionization electrode material with high desalination capacity: experiment and simulation. *Int. J. Environ. Res. Public Health*, 20, 517. DOI: 10.3390/ijerph20010517.

JLL, 2024. Utility-scale battery storage opens up for investors. Available at: https://www.jll.com/en-us/insights/utility-scale-battery-storage-opens-up-for-investors.

Jung S.C., Jung D.S., Choi J.W., Han Y.-K., 2014. Atom-level understanding of the sodiation process in silicon anode material. *J. Phys. Chem. Lett.*, 5, 1283–1288. DOI: 10.1021/jz5002743.

Kehne P., Guhl C., Ma Q., Tietz F., Alff L., Hausbrand R., Komissinskiy P., 2019. Electrochemical performance of all-solid-state sodium-ion model cells with crystalline Na_xCoO_2 thin-film cathodes. *J. Electrochem. Soc.*, 166, A5328. DOI: 10.1149/2.0491903jes.

Kim H., Sadan M.K., Kim C., Choi G.-I., Seong M., Cho K.-K., Kim K.-W., Ahn J.-H., Ahn H.-J., 2021. Electrochemical properties of flexible anode with SnO_2 nanopowder for sodium-ion batteries. *Arch. Metall. Mater.*, 66, 931–934. DOI: 10.24425/AMM.2021.136399.

Kim J., Han S.-D., Koo B., Lee S.-H., Yang J., 2023. Structure dependent electrochemical behaviors of hard carbon anode materials derived from natural polymer for next-generation sodium ion battery. *Polymers*, 15, 4373. DOI: 10.3390/polym15224373.

Kim S.-B., Lee S.-H., 2024. Application of deep learning techniques for the state of charge prediction of lithium-ion batteries. *Appl. Sci.*, 14, 8077. DOI: 10.3390/app14178077.

Kittner N., Lill F., Kammen D.M., 2017. Energy storage deployment and innovation for the clean energy transition. *Nat. Energy*, 2, 17125. DOI: 10.1038/nenergy.2017.125.

Koech A.K., Mwandila G., Mulolani F., Mwaanga P., 2024. Lithium-ion battery fundamentals and exploration of cathode materials: a review. *S. Afr. J. Chem. Eng.*, 50, 321–339. DOI: 10.1016/j.sajce.2024.09.008.

Koketsu T., Ma J., Morgan B.J., Body M., Legein C., Dachraoui W., Giannini M., Demortière A., Salanne M., Dardoize F., Groult H., Borkiewicz O.J., Chapman K.W., Strasser P., Dambournet D., 2017. Reversible magnesium and aluminium ions insertion in cation-deficient anatase TiO_2. *Nat. Mater.*, 16, 1142–1148. DOI: 10.1038/NMAT4976.

Komaba S., Hasegawa T., Dahbi M., Kubota K., 2015. Potassium intercalation into graphite to realize high-voltage/high-power potassium-ion batteries and potassium-ion capacitors. *Electrochem. Commun.*, 60, 172–175. DOI: 10.1016/j.elecom.2015.09.002.

Komarnicki P., 2016. Energy storage systems: power grid and energy market use cases. *Arch. Electr. Eng.*, 65, 495–511. DOI: 10.1515/AEE-2016-0036.

Kubota K., Dahbi M., Hosaka T., Kumakura S., Komaba S., 2018. Towards K-ion and Na-ion batteries as 'beyond Li-ion'. *Chem. Rec.*, 18, 459–479. DOI: 10.1002/tcr.201700057.

Kubota K., Ikeuchi I., Nakayama T., Takei C., Yabuuchi N., Shiiba H., Nakayama M., Komaba S., 2015. New insight into structural evolution in layered $NaCrO_2$ during electrochemical sodium extraction. *J. Phys. Chem. C*, 119, 166–175. DOI: 10.1021/jp5105888.

Kujawińska A., Hamrol A., Brzozowski K., 2022. Minimizing the emission of material waste in the production process of batteries. *Bull. Pol. Acad. Sci. Tech. Sci.*, 70, e144049. DOI: 10.24425/BPASTS.2022.144049.

Lavanya N., Sahaya Dennish Babu G., Judith Jayarani A., Prithivirajan P., Ayeshamariam A., 2025. Chapter 1 - Introduction and history of lithium-ion batteries, In: Thomas S., Gueye A.B., Savadogo O., Maria H.J. (Eds.), *Nanostructured lithium-ion battery materials: Synthesis, characterization, and applications*. Elsevier, 3–20. DOI: 10.1016/B978-0-443-13338-1.00016-2.

Lei Y., Li X., Liu L., Ceder G., 2014. Synthesis and stoichiometry of different layered sodium cobalt oxides. *Chem. Mater.*, 26, 5288–5296. DOI: 10.1021/cm5021788.

Leonova A.M., Bashirov O.A., Leonova N.M., Lebedev A.S., Trofimov A.A., Suzdaltsev A.V, 2023. Synthesis of C/SiC mixtures for composite anodes of lithium-ion power sources. *Appl. Sci.*, 13, 901. DOI: 10.3390/app13020901.

Levi E., Mitelman A., Isnard O., Brunelli M., Aurbach D., 2008. Phase diagram of Mg insertion into Chevrel phases, $Mg_xMo_6T_8$ (T = S, Se). 3. The crystal structure of triclinic $Mg_2Mo_6Se_8$. *Inorg. Chem.*, 47, 1975–1983. DOI: 10.1021/ic702311f.

Li C., Jiang W.-J., Liu Z.-Y., 2024. Carbon nanofibers-based anodes for potassium-ion battery. *ChemistryOpen*, 13, e202300286. DOI: 10.1002/open.202300286.

Li Y., Lu Y., Adelhelm P., Titirici M.-M., Hu Y.-S., 2019. Intercalation chemistry of graphite: alkali metal ions and beyond. *Chem. Soc. Rev.*, 48, 4655–4687. DOI: 10.1039/c9cs00162j.

Li Y., Ma J., Yin J., Xu J., Wei X., Hu Z., Chen W., Hu F., Yue C., 2026. Flexible lithium-ion batteries with LCO cathodes: recent advances and perspectives. *Nano Energy*, 148, 111644. DOI: 10.1016/j.nanoen.2025.111644.

Limachi C., Rogala K., Broszkiewicz M., Cabello M., Niedzicki L., Armand M., Wieczorek W., 2024. Development of fluorine-free electrolytes for aqueous-processed olivine-type phosphate cathodes. *Molecules*, 29, 4698. DOI: 10.3390/molecules29194698.

Lindagato P., Li Y., Macháček J., Yang G., Mungwarakarama I., Ndahimana A., Kanimba Ntwali H.P., 2023. Lithium metal: the key to green transportation. *Appl. Sci.*, 13, 405. DOI: 10.3390/app13010405.

Ling C., Zhang R., 2017. Manganese dioxide as rechargeable magnesium battery cathode. *Front. Energy Res.,* 5, 30. DOI: 10.3389/fenrg.2017.00030.

Lipson A.L., Pan B., Lapidus S.H., Liao C., Vaughey J.T., Ingram B.J., 2015. Rechargeable Ca-ion batteries: a new energy storage system. *Chem. Mater.*, 27, 8442–8447. DOI: 10.1021/ACS.CHEMMATER.5B04027.

Liu D., Palmore G.T.R., 2017. Synthesis, crystal structure, and electrochemical properties of alluaudite $Na_{1.702}Fe_3(PO_4)_3$ as a sodium-ion battery cathode. *ACS Sustainable Chem. Eng.*, 5, 5766–5771. DOI: 10.1021/acssuschemeng.7b00371.

Liu F., Cheng X., Xu R., Wu Y., Jiang Y., Yu Y., 2018. Binding sulfur-doped Nb_2O_5 hollow nanospheres on sulfur-doped graphene networks for highly reversible sodium storage. *Adv. Funct. Mater.*, 28, 1800394. DOI: 10.1002/adfm.201800394.

Liu S.-W., Niu B.-T., Lin B.-L., Lin Y.-T., Chen X.-P., Guo H.-X., Chen Y.-X., Lin X.-M., 2024. Investigating the electrochemical performance of $MnFe_2O_4$@xC nanocomposites as anode materials for sodium-ion batteries. *Molecules*, 29, 3912. DOI: 10.3390/molecules29163912.

Lung L.-Y., Chou T.-Y., Chang W.-C., Kuo C.-C., 2023. Development of energy storage systems for high penetration of renewable energy grids. *Appl. Sci.*, 13, 11978. DOI: 10.3390/app132111978.

Lung-Hao Hu B., Wu F.-Y., Lin C.-T., Khlobystov A.N., Li L.-J., 2013. Graphene-modified $LiFePO_4$ cathode for lithium ion battery beyond theoretical capacity. *Nat. Commun.*, 4, 1687. DOI: 10.1038/ncomms2705.

Luo L., Zhen Y., Lu Y., Zhou K., Huang J., Huang Z., Mathur S., Hong Z., 2020. Structural evolution from layered $Na_2Ti_3O_7$ to $Na_2Ti_6O_{13}$ nanowires enabling a highly reversible anode for Mg-ion batteries. *Nanoscale*, 12, 230–238. DOI: 10.1039/c9nr08003a.

Ma Y., Liu W., Liu W., Zhang G., Wang Y., Wang H., Chen W., Huang M., Wang X., 2024. Coconut-solid-waste-derived hard-carbon anode materials for fast potassium ion storage. *Coatings*, 14, 208. DOI: 10.3390/coatings14020208.

Maltsev A.P., Chepkasov I.V., Oganov A.R., 2024. New promising class of anode materials for Ca-ion battery: polyaromatic hydrocarbons. *Mater. Today Energy*, 39, 101467. DOI: 10.1016/J.MTENER.2023.101467.

Manthiram A., 2017. An outlook on lithium ion battery technology. *ACS Cent. Sci.*, 3, 1063–1069. DOI: 10.1021/acscentsci.7b00288.

Mao M., Lin Z., Tong Y., Yue J., Zhao C., Lu J., Zhang Q., Gu L., Suo L., Hu Y.-S., Li H., Huang X., Chen L., 2020. Iodine vapor transport-triggered preferential growth of Chevrel Mo_6S_8 nanosheets for advanced multivalent batteries. *ACS Nano*, 14, 1102–1110. DOI: 10.1021/acsnano.9b08848.

Masese T., Kanyolo G.M., 2023. Advancements in cathode materials for potassium-ion batteries: current landscape, obstacles, and prospects. *Energy Adv.*, 3, 60–107. DOI: 10.1039/d3ya00406f.

Medina A., Pérez-Vicente C., Alcántara R., 2021. Advancing towards a practical magnesium ion battery. *Materials*, 14, 7488. DOI: 10.3390/ma14237488.

Mizushima K., Jones P.C., Wiseman P.J., Goodenough J.B., 1980. Li_xCoO_2 ($0 < x < 1$): a new cathode material for batteries of high energy density. *Mater. Res. Bull.*, 15, 783–789. DOI: 10.1016/0025-5408(80)90012-4.

Mousavian S.M.H., Bautin V.A., 2025. Rechargeable magnesium batteries: overcoming challenges for high-efficiency energy applications. *J. Energy Storage*, 126, 117079. DOI: 10.1016/j.est.2025.117079.

Mu K., Mu Y., Wang X., Wu X., Pang C., Huang Y.-T., Feng S.-P., 2022. Direct thermal charging cell using nickel hexacyanoferrate (II) anode for green recycling of low-grade heat. *ACS Energy Lett.*, 7, 1146–1153. DOI: 10.1021/acsenergylett.2c00057.

Nandihalli N., Chouhan R.K., Kuchi R., Hlova I.Z., 2024. Aspects of spodumene lithium extraction techniques. *Sustainability*, 16, 8513. DOI: 10.3390/su16198513.

Nathan M.G.T., Yu H., Kim G.T., Kim J.H., Cho J.S., Kim J., Kim J.K., 2022. Recent advances in layered metal-oxide cathodes for application in potassium-ion batteries. *Adv. Sci.*, 9, 2105882. DOI: 10.1002/advs.202105882.

Nazarov A., Sulimin V., Shvedov V., 2024. Renewable energy sources: global implementation experience. *E3S Web Conf.*, 474, 01030. DOI: 10.1051/e3sconf/202447401030.

Nekahi A., Dorri M., Rezaei M., Bouguern M.D., Madikere Raghunatha Reddy A.K., Li X., Deng S., Zaghib K., 2024. Comparative issues of metal-ion batteries toward sustainable energy storage: lithium vs. sodium. *Batteries*, 10, 279. DOI: 10.3390/batteries10080279.

Nelson P.A., Gallagher K.G., Bloom I., Dees D.W., 2011. Modeling the performance and cost of lithium-ion batteries for electric-drive vehicles. Argonne National Laboratory. Avaiable at: https://publications.anl.gov/anlpubs/2011/10/71302.pdf.

Ni J., Li L., Lu J., 2018. Phosphorus: an anode of choice for sodium-ion batteries. *ACS Energy Lett.*, 3, 1137–1144. DOI: 10.1021/acsenergylett.8b00312.

Nitta N., Wu F., Lee J.T., Yushin G., 2015. Li-ion battery materials: present and future. *Mater. Today*, 18, 252–264. DOI: 10.1016/j.mattod.2014.10.040.

Niu J., Zhang Z., Aurbach D., 2020. Alloy Anode Materials for Rechargeable Mg Ion Batteries. *Adv. Energy Mater.*, 2000697. DOI: 10.1002/aenm.202000697.

Nowaczek A., Kulczycka J., 2020. Overview of funding sources and technologies for the recovery of raw materials from spent batteries and rechargeable batteries in Poland. *Gospod. Surowcami Miner. – Miner. Resour. Manage.*, 36, 153–172. DOI: 10.24425/gsm.2020.132564.

Nowak A.P., Rutecki P., Szkoda M., Trzciński K., 2024. Determination of sodium ion diffusion coefficient in tin sulfide@carbon anode material using GITT and EIS techniques. *Energies*, 17, 3233. DOI: 10.3390/en17133233.

Overhoff G.M., Nölle R., Siozios V., Winter M., Placke T., 2021. A thorough analysis of two different pre-lithiation techniques for silicon/carbon negative electrodes in lithium ion batteries. *Batteries Supercaps*, 4, 1163–1174. DOI: 10.1002/batt.202100024.

Padhi A.K., Nanjundaswamy K.S., Goodenough J.B., 1997. Phospho-olivines as positive-electrode materials for rechargeable lithium batteries. *J. Electrochem. Soc.*, 144, 1188. DOI: 10.1149/1.1837571.

Palumbo O., 2023. Innovative materials for batteries. *Appl. Sci.*, 13, 7595. DOI: 10.3390/app13137595.

Pan H., Zheng K., Chen Z., Wang Y., Tan Y., Wang J., Yao L., Wang L., Sun C., Yang J., 2024. Tuning the electronic structures of Mo-based sulfides/selenides with biomass-derived carbon for hydrogen evolution reaction and sodium-ion batteries. *Catalysts*, 14, 627. DOI: 10.3390/catal14090627.

Park J., Kim J., Kim J., Kim M., Song T., Paik U., 2025. Sustainable and cost-effective electrode manufacturing for advanced lithium batteries: the roll-to-roll dry coating process. *Chem. Sci.*, 16, 6598–6619. DOI: 10.1039/d5sc00059a.

Passerini S., Barelli L., Baumann M.J., Peters J.F., 2024. *Emerging battery technologies to boost the clean energy transition: cost, sustainability, and performance analysis*. Springer Cham. DOI: 10.1007/978-3-031-48359-2.

Ponrouch A., Frontera C., Bardé F., Palacín M.R., 2016. Towards a calcium-based rechargeable battery. *Nat. Mater.*, 15, 169–172. DOI: 10.1038/nmat4462.

Qian G., Wang J., Li H., Ma Z.-F., Pianetta P., Li L., Yu X., Liu Y., 2022. Structural and chemical evolution in layered oxide cathodes of lithium-ion batteries revealed by synchrotron techniques. *Natl. Sci. Rev.*, 9, nwab146. DOI: 10.1093/nsr/nwab146.

Richard J., Benayad A., Colin J.-F., Martinet S., 2017. Charge transfer mechanism into the Chevrel phase Mo_6S_8 during Mg intercalation. *J. Phys. Chem. C*, 121, 17096–17103. DOI: 10.1021/acs.jpcc.7b03979.

Roberts M.B., Bruce A., MacGill I., 2019. Impact of shared battery energy storage systems on photovoltaic self-consumption and electricity bills in apartment buildings. *Appl. Energy*, 245, 78–95. DOI: 10.1016/j.apenergy.2019.04.001.

Roy J.J., Phuong D.M., Verma V., Chaudhary R., Carboni M., Meyer D., Cao B., Srinivasan M., 2024. Direct recycling of Li-ion batteries from cell to pack level: challenges and prospects on technology, scalability, sustainability, and economics. *Carbon Energy*, 6, e492. DOI: 10.1002/cey2.492.

Royal Society of Chemistry. *Calcium*. RSC Periodic Table. Available at: https://periodic-table.rsc.org/element/20/calcium.

Saint J.A., Doeff M.M., Wilcox J., 2008. Electrode materials with the $Na_{0.44}MnO_2$ structure: effect of titanium substitution on physical and electrochemical properties. *Chem. Mater.*, 20, 3404–3411. DOI: 10.1021/cm800247u.

Sakaushi K., Hosono E., Nickerl G., Gemming T., Zhou H., Kaskel S., Eckert J., 2013. Aromatic porous-honeycomb electrodes for a sodium-organic energy storage device. *Nat. Commun.*, 4, 1485. DOI: 10.1038/ncomms2481.

Sangsanit T., Matkhaw N., Benwannamas N., Songthan R., Tejangkura W., Sawangphruk M., 2025. Layered lithium- and manganese-rich oxide cathode cells in large-scale cylindrical configuration: optimized electrolyte formulations with LiDFOB and $LiBF_4$ Co-additives for enhanced stability. *J. Power Sources*, 632, 236337. DOI: 10.1016/j.jpowsour.2025.236337.

Sauvage F., Laffont L., Tarascon J.-M., Baudrin E., 2007. Study of the insertion/deinsertion mechanism of sodium into $Na_{0.44}MnO_2$. *Inorg. Chem.*, 46, 3289–3294. DOI: 10.1021/ic0700250.

Schirber M., 2024. Sodium as a green substitute for lithium in batteries. *Physics*, 17, 73. DOI: 10.1103/physics.17.73.

Sgourou E.N., Daskalopulu A., Tsoukalas L.H., Goulatis I.L., Vovk R.V., Chroneos A., 2023. Kinetics of ions in post-lithium batteries. *Appl. Sci.*, 13, 9619. DOI: 10.3390/app13179619.

Shah R., Mittal V., Matsil E., Rosenkranz A., 2021. Magnesium-ion batteries for electric vehicles: current trends and future perspectives. *Adv. Mech. Eng.* 13, 1–9 DOI: 10.1177/16878140211003398.

Shahabuddin M., Alim M.A., Alam T., Mofijur M., Ahmed S.F., Perkins G., 2021. A critical review on the development and challenges of concentrated solar power technologies. *Sustainable Energy Technol. Assess.*, 47, 101434. DOI: 10.1016/j.seta.2021.101434.

Shahid S., Agelin-Chaab M., 2023. Chapter 10 – Battery thermal management through simulation and experiment: Air cooling and enhancement, In: Aloui F., Varuvel E.G., Sonthalia A. (Eds.), Handbook of Thermal Management Systems. Elsevier, 221–254. DOI: 10.1016/B978-0-443-19017-9.00008-8.

Shao Y., Gu M., Li X., Nie Z., Zuo P., Li G., Liu T., Xiao J., Cheng Y., Wang C., Zhang J.-G., Liu J., 2014. Highly reversible Mg insertion in nanostructured Bi for Mg ion batteries. *Nano Lett.*, 14, 255–260. DOI: 10.1021/nl403874y.

Shibata T., Fukuzumi Y., Kobayashi W., Moritomo Y., 2015. Fast discharge process of layered cobalt oxides due to high Na^+ diffusion. *Sci. Rep.*, 5, 9006. DOI: 10.1038/srep09006.

Shim H.-W., Im B., Joo S., Kim D.-G., 2024. Facile synthesis and Li-electroactivity of cobalt oxide based on resources recovered from waste lithium-ion batteries. *Arch. Metall. Mater.*, 69, 67–72. DOI: 10.24425/AMM.2024.147787.

Stournara M.E., Shenoy V.B., 2011. Enhanced Li capacity at high lithiation potentials in graphene oxide. *J. Power Sources*, 196, 5697–5703. DOI: 10.1016/j.jpowsour.2011.02.024.

Su D., Dou S., Wang G., 2015. Bismuth: a new anode for the Na-ion battery. *Nano Energy*, 12, 88–95. DOI: 10.1016/j.nanoen.2014.12.012.

Sun X., Duffort V., Mehdi B.L., Browning N.D., Nazar L.F., 2016. Investigation of the mechanism of Mg insertion in birnessite in nonaqueous and aqueous rechargeable Mg-ion batteries. *Chem. Mater.*, 28, 534–542. DOI: 10.1021/acs.chemmater.5b03983.

Tan Y.-H., Yao W.-T., Zhang T., Ma T., Lu L.-L., Zhou F., Yao H.-B., Yu S.-H., 2018. High voltage magnesium-ion battery enabled by nanocluster Mg*3*Bi*2* alloy anode in noncorrosive electrolyte. *ACS Nano*, 12, 5856–5865. DOI: 10.1021/acsnano.8b01847.

Tepavcevic S., Liu Y., Zhou D., Lai B., Maser J., Zuo X., Chan H., Král P., Johnson C.S., Stamenkovic V., Markovic N.M., Rajh T., 2015. Nanostructured layered cathode for rechargeable Mg-ion batteries. *ACS Nano*, 9, 8194–8205. DOI: 10.1021/acsnano.5b02450.

Thackeray M.M., 1999. Spinel electrodes for lithium batteries. *J. Am. Ceram. Soc.*, 82, 3347–3354. DOI: 10.1111/j.1151-2916.1999.tb02250.x.

Tinker H.R., Howard C.A., Zhou M., Xu Y., 2023. Exploring anodes for calcium-ion batteries. *Mater. Adv.*, 4, 2028–2041. DOI: 10.1039/D2MA01034H.

Tolstoy V.P., Vladimirova N.I., Gulina L.B., 2019. Formation of ordered honeycomb-like structures of manganese oxide 2D nanocrystals with the birnessite-like structure and their electrocatalytic properties during oxygen evolution reaction upon water splitting in an alkaline medium. *ACS Omega*, 4, 22203–22208. DOI: 10.1021/acsomega.9b03499.

U.S. Geological Survey, 2020. Mineral Commodity Summaries 2020. U.S. Geological Survey, Reston, Virginia. DOI: https://doi.org/10.3133/mcs2020.

Vieira F.M., Moura P.S., de Almeida A.T., 2017. Energy storage system for self-consumption of photovoltaic energy in residential zero energy buildings. *Renewable Energy*, 103, 308–320. DOI: 10.1016/j.renene.2016.11.048.

Wahid M., Puthusseri D., Gawli Y., Sharma N., Ogale S., 2018. Hard carbons for sodium-ion battery anodes: synthetic strategies, material properties, and storage mechanisms. *ChemSusChem*, 11, 506–526. DOI: 10.1002/cssc.201701664.

Waldmann T., Scurtu R.-G., Richter K., Wohlfahrt-Mehrens M., 2020. 18650 vs. 21700 Li-ion cells – a direct comparison of electrochemical, thermal, and geometrical properties. *J. Power Sources*, 472, 228614. DOI: 10.1016/j.jpowsour.2020.228614.

Wan L.F., Incorvati J.T., Poeppelmeier K.R., Prendergast D., 2016. Building a fast lane for Mg diffusion in α-MoO_3 by fluorine doping. *Chem. Mater.*, 28, 6900–6908. DOI: 10.1021/acs.chemmater.6b02223.

Wang B., Deng T., Liu J., Sun B., Su Y., Ti R., Shangguan L., Zhang C., Tang Y., Cheng N., Xu Y., Guo J., 2024. Scaly MoS_2/rGO composite as an anode material for high-performance potassium-ion battery. *Molecules*, 29, 2977. DOI: 10.3390/molecules29132977.

Wang G., Xiong X., Xie D., Lin Z., Zheng J., Zheng F., Li Y., Liu Y., Yang C., Liu M., 2018a. Chemically activated hollow carbon nanospheres as a high-performance anode material for potassium ion batteries. *J. Mater. Chem. A*, 6, 24317–24323. DOI: 10.1039/c8ta09751h.

Wang J., Wang J., Jiang Y., Xiong F., Tan S., Qiao F., Chen J., An Q., Mai L., 2022. $CaV_6O_{16}{\cdot}2.8H_2O$ with Ca^{2+} pillar and water lubrication as a high-rate and long-life cathode material for Ca-ion batteries. *Adv. Funct. Mater.*, 32, 2113030. DOI: 10.1002/ADFM.202113030.

Wang L., Welborn S.S., Kumar H., Li M., Wang Z., Shenoy V.B., Detsi E., 2019. High-rate and long cycle-life alloy-type magnesium-ion battery anode enabled through (de)magnesiation-induced near-room-temperature solid–liquid phase transformation. *Adv. Energy Mater.*, 9, 1902086. DOI: 10.1002/aenm.201902086.

Wang R.Y., Wessells C.D., Huggins R.A., Cui Y., 2013. Highly reversible open framework nanoscale electrodes for divalent ion batteries. *Nano Lett.*, 13, 5748–5752. DOI: 10.1021/NL403669A.

Wang W., Liu L., Wang P.-F., Zuo T.-T., Yin Y.-X., Wu N., Zhou J.-M., Wei Y., Guo Y.-G., 2018b. A novel bismuth-based anode material with a stable alloying process by the space confinement of an in situ conversion reaction for a rechargeable magnesium ion battery. *Chem. Commun.*, 54, 1714–1717. DOI: 10.1039/c7cc08206a.

Wang X., Kajiyama S., Iinuma H., Hosono E., Oro S., Moriguchi I., Okubo M., Yamada A., 2015. Pseudocapacitance of MXene nanosheets for high-power sodium-ion hybrid capacitors. *Nat. Commun.*, 6, 6544. DOI: 10.1038/ncomms7544.

Wei L., Ji D., Zhao F., Tian X., Guo Y., Yan J., 2024. A review of carbon nanofiber materials for dendrite-free lithium-metal anodes. *Molecules*, 29, 4096. DOI: 10.3390/molecules29174096.

Wen Y., He K., Zhu Y., Han F., Xu Y., Matsuda I., Ishii Y., Cumings J., Wang C., 2014. Expanded graphite as superior anode for sodium-ion batteries. *Nat. Commun.*, 5, 4033. DOI: 10.1038/ncomms5033.

Wentker M., Greenwood M., Leker J., 2019. A bottom-up approach to lithium-ion battery cost modeling with a focus on cathode active materials. *Energies*, 12, 504. DOI: 10.3390/en12030504.

Wessells C.D., Huggins R.A., Cui Y., 2011a. Copper hexacyanoferrate battery electrodes with long cycle life and high power. *Nat. Commun.*, 2, 550. DOI: 10.1038/ncomms1563.

Wessells C.D., Peddada S.V., Huggins R.A., Cui Y., 2011b. Nickel hexacyanoferrate nanoparticle electrodes for aqueous sodium and potassium ion batteries. *Nano Lett.*, 11, 5421–5425. DOI: 10.1021/NL203193Q.

Whittingham M.S., 1976. Electrical energy storage and intercalation chemistry. *Science*, 192, 1126–1127. DOI: 10.1126/science.192.4244.1126.

Winter M., Barnett B., Xu K., 2018. Before Li ion batteries. *Chem. Rev.*, 118, 11433–11456. DOI: 10.1021/acs.chemrev.8b00422.

Wood W.W., Smedley P.L., Lindsey B.D., Wood W.T., Kirchheim R.E., Cherry J.A., 2022. Global groundwater solute composition and concentrations. *Groundwater*, 60, 714–720. DOI: 10.1111/GWAT.13205.

Wu Q., Shu K., Zhao L., Zhang J., 2024. Pomegranate peel-derived hard carbons as anode materials for sodium-ion batteries. *Molecules*, 29, 4639. DOI: 10.3390/molecules29194639.

Wu Y., Song T.-Y., Chen L.-N., 2021. A review on recent developments of vanadium-based cathode for rechargeable zinc-ion batteries. *Tungsten*, 3, 289–304. DOI: 10.1007/s42864-021-00091-9.

Xiang X., Zhang K., Chen J., 2015. Recent advances and prospects of cathode materials for sodium-ion batteries. *Adv. Mater.*, 27, 5343–5364. DOI: 10.1002/adma.201501527.

Xie J., Lu Y.-C., 2020. A retrospective on lithium-ion batteries. *Nat. Commun.*, 11, 2499. DOI: 10.1038/s41467-020-16259-9.

Xu L., Wang S., Xi L., Li Y., Gao J., 2024. A review of thermal management and heat transfer of lithium-ion batteries. *Energies*, 17, 3873. DOI: 10.3390/en17163873.

Xu M., Niu Y., Chen C., Song J., Bao S., Li C.M., 2014. Synthesis and application of ultra-long $Na_{0.44}MnO_2$ submicron slabs as a cathode material for Na-ion batteries. *RSC Adv.*, 4, 38140–38143. DOI: 10.1039/c4ra07355j.

Xu S., Dong H., Yang D., Wu C., Yao Y., Rui X., Chou S.-L., Yu Y., 2023. Promising cathode materials for sodium-ion batteries from lab to application. *ACS Cent. Sci.*, 9, 2012–2035. DOI: 10.1021/acscentsci.3c01022.

Xu X., Duan M., Yue Y., Li Q., Zhang X., Wu L., Wu P., Song, B., Mai L., 2019. Bilayered $Mg_{0.25}V_2O_5{\cdot}H_2O$ as a stable cathode for rechargeable Ca-ion batteries. *ACS Energy Lett.*, 4, 1328–1335. DOI: 10.1021/ACSENERGYLETT.9B00830.

Yang X.-G., Liu T., Wang C.-Y., 2021. Thermally modulated lithium iron phosphate batteries for mass-market electric vehicles. *Nat. Energy*, 6, 176–185. DOI: 10.1038/s41560-020-00757-7.

Yang Y., Wang R., Shen Z., Yu Q., Xiong R., Shen W., 2023. Towards a safer lithium-ion batteries: a critical review on cause, characteristics, warning and disposal strategy for thermal runaway. *Adv. Appl. Energy*, 11, 100146. DOI: 10.1016/j.adapen.2023.100146.

Yin Z., Wu J., Tian Y., Yuan Y., Gu M., Cheng L., Wang Y., Kim Y., 2025. High-performance quasi-solid-state calcium-ion batteries from redox-active covalent organic framework electrolytes. *Adv. Sci.*, 13, e12328. DOI: 10.1002/advs.202512328.

Ying H., Han W.-Q., 2017. Metallic Sn-based anode materials: application in high-performance lithium-ion and sodium-ion batteries. *Adv. Sci.*, 4, 1700298. DOI: 10.1002/advs.201700298.

Yuan L.-X., Wang Z.-H., Zhang W.-X., Hu X.-L., Chen J.-T., Huang Y.-H., Goodenough J.B., 2011. Development and challenges of LiFePO*4* cathode material for lithium-ion batteries. *Energy Environ. Sci.*, 4, 269–284. DOI: 10.1039/c0ee00029a.

Yüksek G., Lale T., 2024. Improved thermal management of lithium-based batteries employing genetic algorithm optimization. *Bull. Pol. Acad. Sci. Tech. Sci.*, 72, e151378. DOI: 10.24425/BPASTS.2024.151378.

Yun S., Liang X., Xi J., Liao L., Cui S., Chen L., Li S., Hu Q., 2024. Electrolytes for high-safety lithium-ion batteries at low temperature: a review. *Polymers*, 16, 2661. DOI: 10.3390/polym16182661.

Zaghib K., Mauger A., Goult H., Goodenough J.B., Julien C.M., 2013. Advanced electrodes for high power Li-ion batteries. *Materials*, 6, 1028–1049. DOI: 10.3390/ma6031028.

Zanoletti A., Carena E., Ferrara C., Bontempi E., 2024. A review of lithium-ion battery recycling: technologies, sustainability, and open issues. *Batteries*, 10, 38. DOI: 10.3390/batteries10010038.

Zeng J., Yang Y., Li C., Li J., Huang J., Wang J., Zhao J., 2017. Li_3VO_4: an insertion anode material for magnesium ion batteries with high specific capacity. *Electrochim. Acta*, 247, 265–270. DOI: 10.1016/j.electacta.2017.06.143.

Zhang J., Miao J., Balasubramani N., Cho D.H., Avey T., Chang C.-Y., Luo A.A., 2023a. Magnesium research and applications: past, present and future. *J. Magnesium Alloys*, 11, 3867–3895. DOI: 10.1016/j.jma.2023.11.007.

Zhang Q., Guo Y., 2025. $MoSe_2$ as a potential anode material for calcium ion batteries: first-principles study. *Mol. Phys.,* 123, e2482680. DOI: 10.1080/00268976.2025.2482680.

Zhang W., Liu Y., Guo Z., 2019a. Approaching high-performance potassium-ion batteries via advanced design strategies and engineering. *Sci. Adv.*, 5, eaav7412. DOI: 10.1126/sciadv.aav7412.

Zhang W., Zhang F., Ming F., Alshareef H.N., 2019b. Sodium-ion battery anodes: status and future trends. *EnergyChem*, 1, 100012. DOI: 10.1016/j.enchem.2019.100012.

Zhang X., Li D., Ruan Q., Liu L., Wang B., Xiong F., Huang C., Chu P.K., 2023b. Vanadium-based cathode materials for rechargeable magnesium batteries. *Mater. Today Energy*, 32, 101232. DOI: 10.1016/j.mtener.2022.101232.

Zhao J., Zhao L., Dimov N., Okada S., Nishida T., 2013. Electrochemical and thermal properties of α-$NaFeO_2$ cathode for Na-ion batteries. *J. Electrochem. Soc.*, 160, A3077. DOI: 10.1149/2.007305jes.

Zhao P.-Y., Zhang S., Choy K.-L., Song Y., Zhang S., Guo D., Yang C., 2025. Silicon negative electrodes for lithium-ion batteries: challenges, advances, and future prospects. *Mater. Horiz.*, 12, 6440–6484. DOI: 10.1039/d5mh00504c.

Zhao Y., Kang Y., Wozny J., Lu J., Du H., Li C., Li T., Kang F., Tavajohi N., Li, B., 2023. Recycling of sodium-ion batteries. *Nat. Rev. Mater.*, 8, 623–634. DOI: 10.1038/s41578-023-00574-w.

Zhao Y., Zhang Z., Zheng Y., Luo Y., Jiang X., Wang Y., Wang Z., Wu Y., Zhang Y., Liu X., Fang B., 2024. Sodium-ion battery at low temperature: challenges and strategies. *Nanomaterials*, 14, 1604. DOI: 10.3390/nano14191604.

Zheng X., Cai Z., Sun J., He J., Rao W., Wang J., Zhang Y., Gao Q., Han B., Xia K., Sun R., Zhou C., 2023. Nickel-rich layered oxide cathodes for lithium-ion batteries: failure mechanisms and modification strategies. *J. Energy Storage*, 58, 106405. DOI: 10.1016/j.est.2022.106405.

Zhou Y.-Y., Zhang Z.-Y., Zhang H.-Z., Li Y., Weng Y., 2021. Progress and perspective of vanadium-based cathode materials for lithium ion batteries. *Tungsten*, 3, 279–288. DOI: 10.1007/S42864-021-00101-W.

Ziegler M.S., Trancik J.E., 2021. Re-examining rates of lithium-ion battery technology improvement and cost decline. *Energy Environ. Sci.*, 14, 1635–1651. DOI: 10.1039/d0ee02681f.